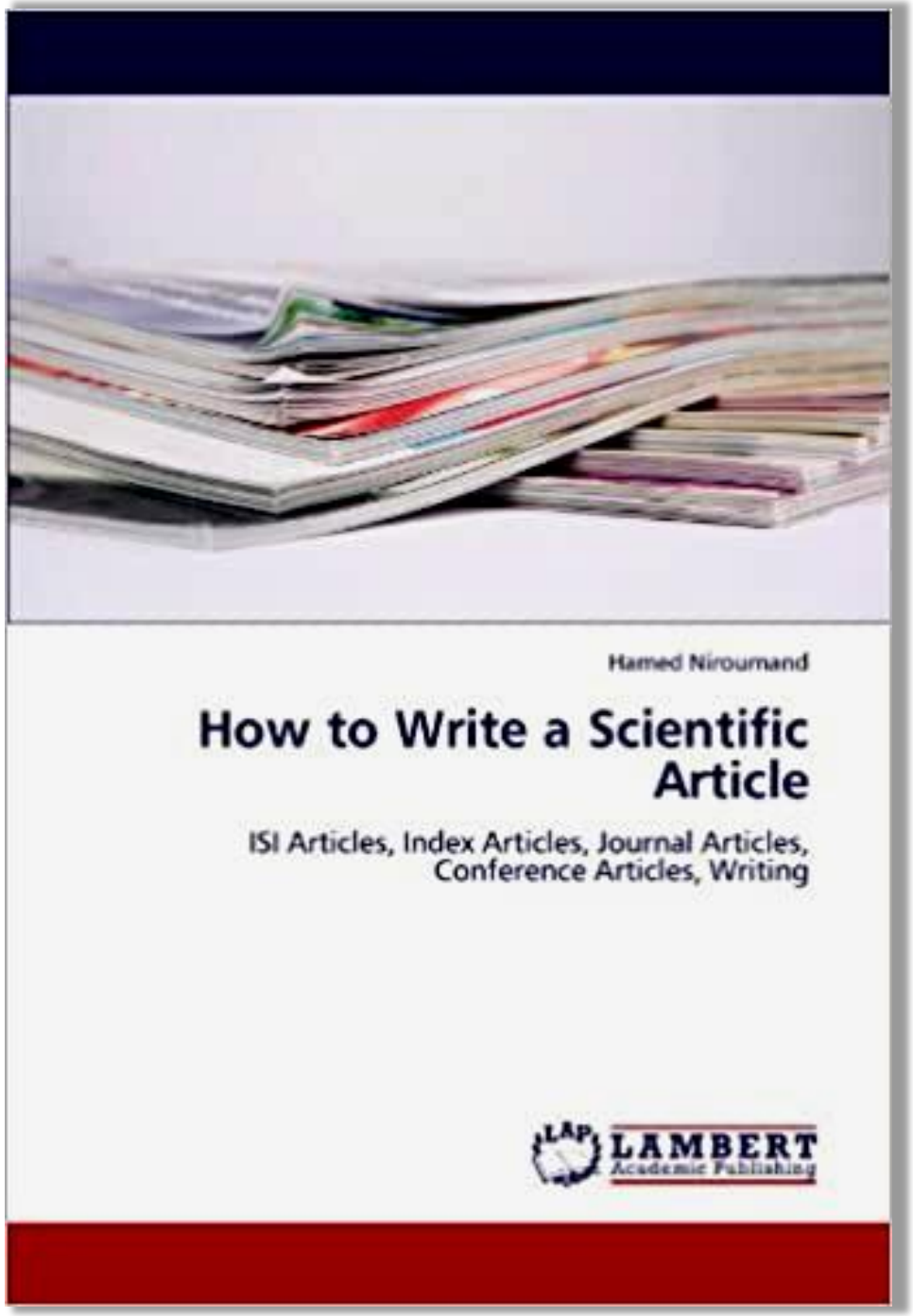
Hamed Niroumand
How to Write a Scientific Article
ISI Articles, Index Articles, Journal Articles, Conference Articles, Writing
LAP
LAMBERT
Academic Publishing

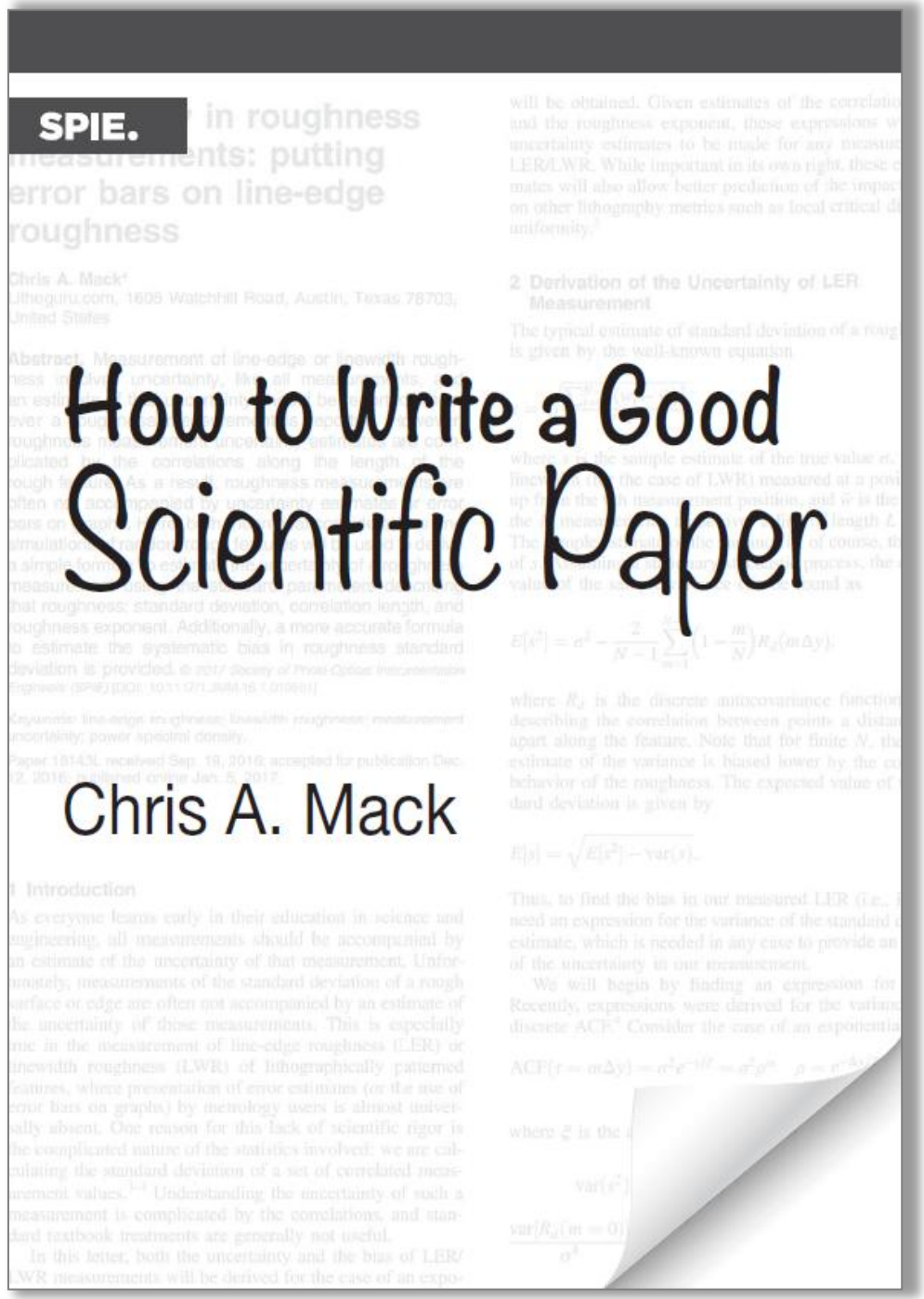
SPIE.
How to Write a Good Scientific Paper
Chris A. Mack

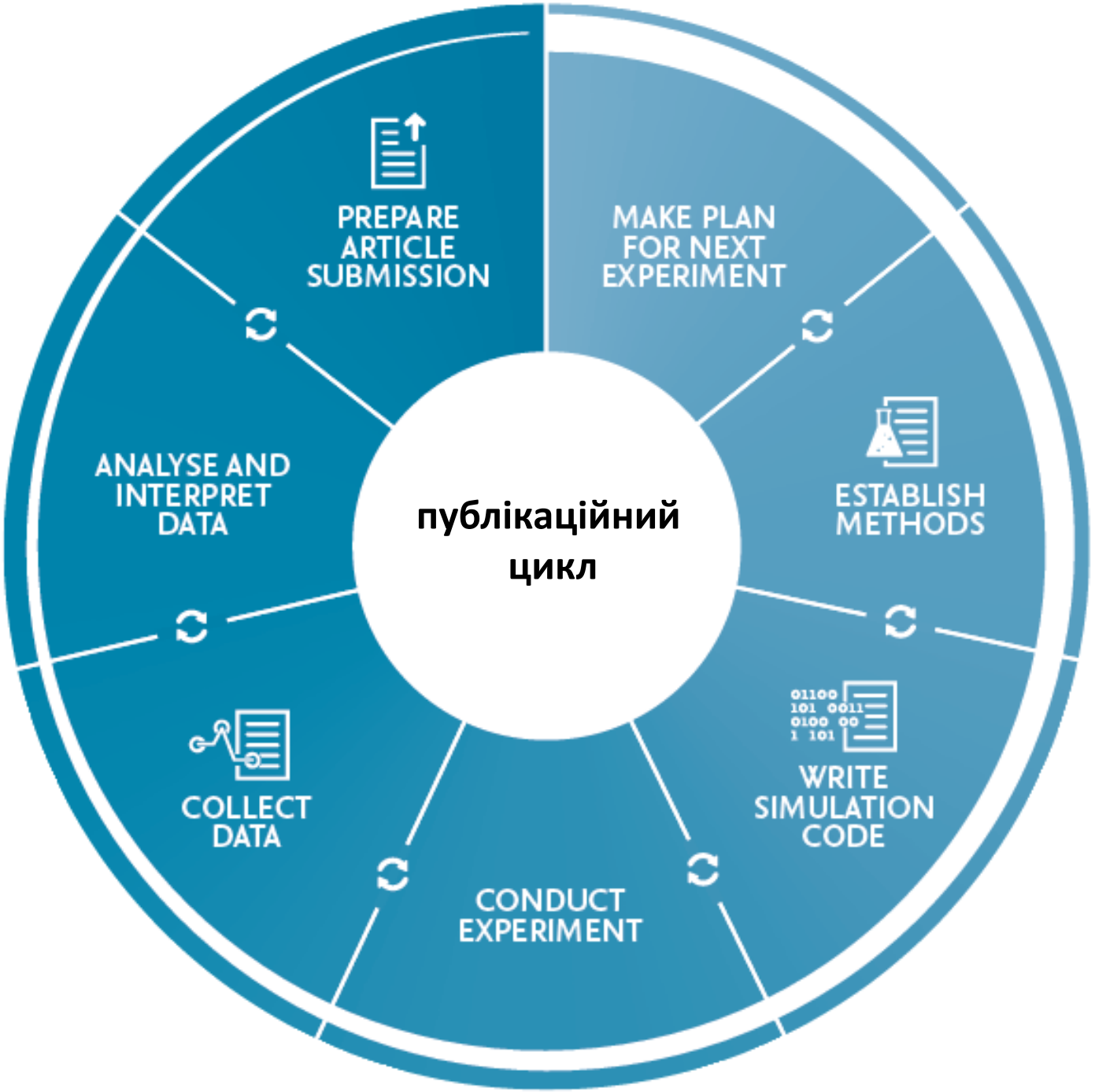
PREPARE ARTICLE SUBMISSION
MAKE PLAN FOR NEXT EXPERIMENT
ESTABLISH METHODS
WRITE SIMULATION CODE
CONDUCT EXPERIMENT
COLLECT DATA
ANALYSE AND INTERPRET DATA
публікаційний цикл

Environmental Science and Pollution Research (2020) 27:26681–26693
https://doi.org/10.1007/s11356-020-09043-1

RESEARCH ARTICLE

Adsorption of Sr(II) ions and salicylic acid onto magnetic magnesium-zinc ferrites: isotherms and kinetic studies

Tetiana Tatarchuk[1,2] · Mu. Naushad[3] · Jolanta Tomaszewska[4] · Przemysław Kosobucki[4] · Mariana Myslin[1] · Hanna Vasylyeva[5] · Piotr Ścigalski[4]

Received: 20 January 2020 / Accepted: 23 April 2020 / Published online: 6 May 2020

Abstract

Magnetic magnesium-zinc spinel ferrite $Mg_{1-x}Zn_xFe_2O_4$ (where $x = 0.4$, 0.6, and 0.8) was investigated as adsorbent for the efficient removal of Sr(II) ions and salicylic acid (SA) contaminants from aqueous medium. The characterization of ferrites was carried out using XRD, VSM, BET, SEM, and EDS. The surface charge of magnetic adsorbents was measured by the drift method. The determination of SA and Sr(II) ion concentrations in the solution phase was carried out by UFLC and complexometry, respectively. It was shown that varying of the Zn(II) content affected the adsorption capacities of magnesium-zinc ferrites. The increasing of zinc content from $x(Zn^{2+}) = 0.4$ to $x(Zn^{2+}) = 0.6$ increased the adsorption of Sr(II) ions from 50 to

article submission:
Tatarchuk, Naushad

концепція: Татарчук, Naushad

титрування: Васільєва
HPLC: Kosobucki+Scigalski

аналіз даних:
Татарчук,
Tomaszewska

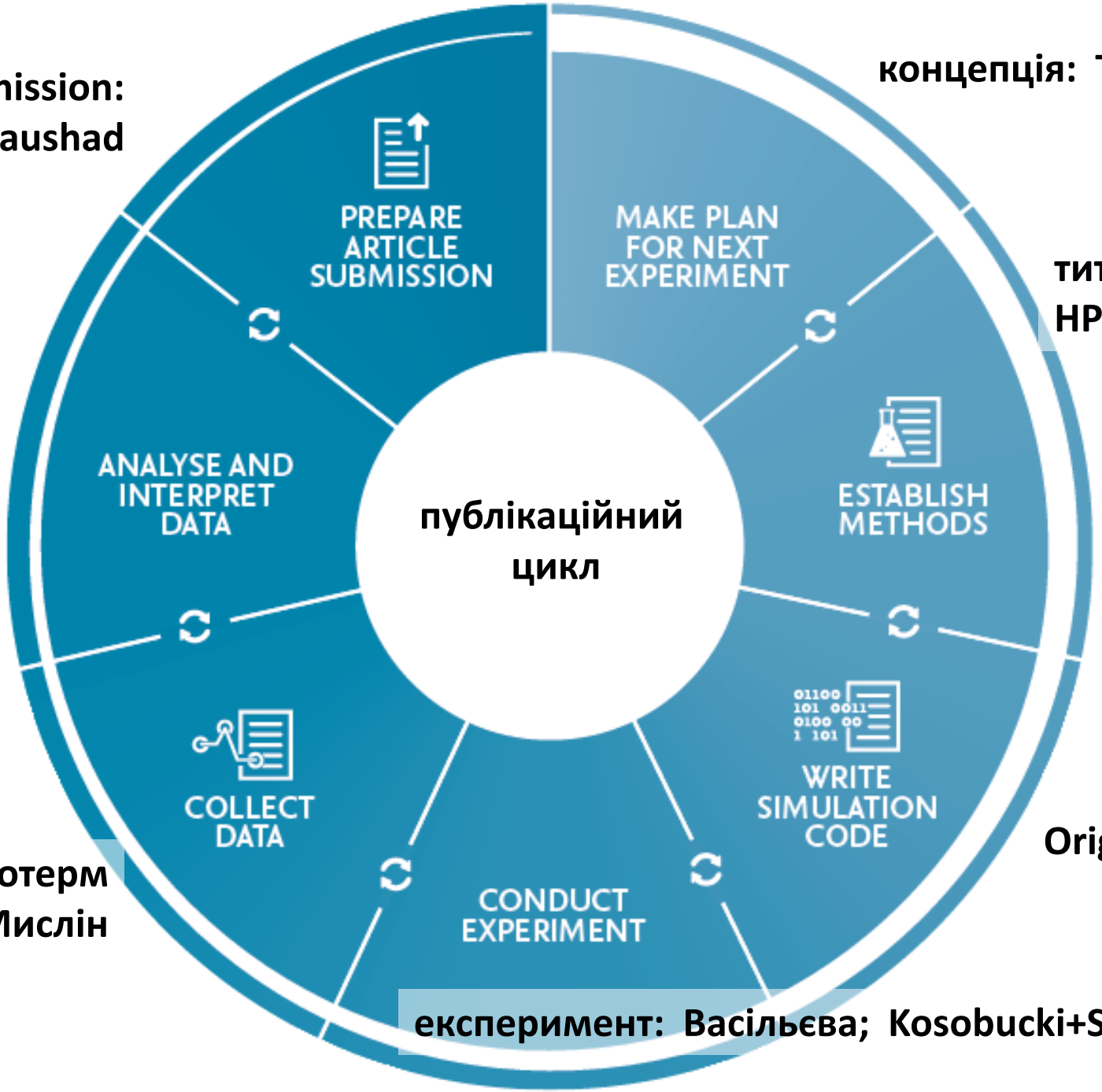

побудова ізотерм
адсорбції: Мислін

Origin: Мислін

експеримент: Васільєва; Kosobucki+Scigalski

The peer review process

науковець робить дослідження

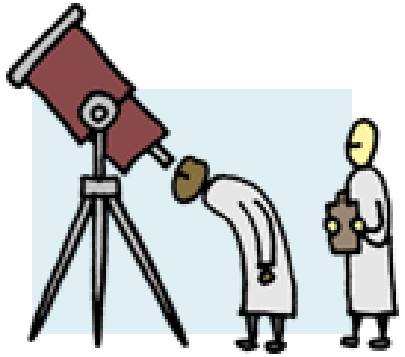

Scientists study something.

редактор надсилає рецензенту (який працює в даній галузі)

науковець пише статтю

Scientists write about their results.

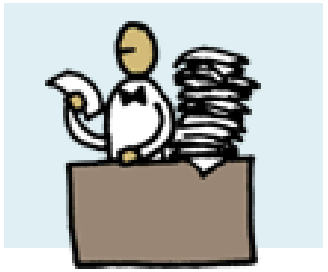

Journal editor receives an article and sends it out for peer review.

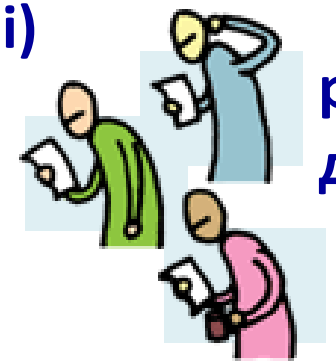

Peer reviewers read the article and provide feedback to the editor.

рецензент дає відгук

науковець покращує зміст статті

Editor may send reviewer comments to the scientists who may then revise and resubmit the article for further review. If an article does not maintain sufficiently high scientific standards, it may be rejected at this point.

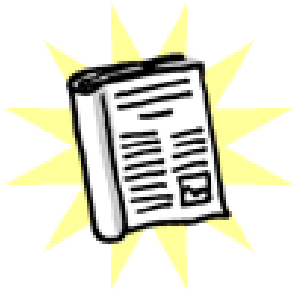

If an article finally meets editorial and peer standards it is published in a journal.

стаття виходить друком

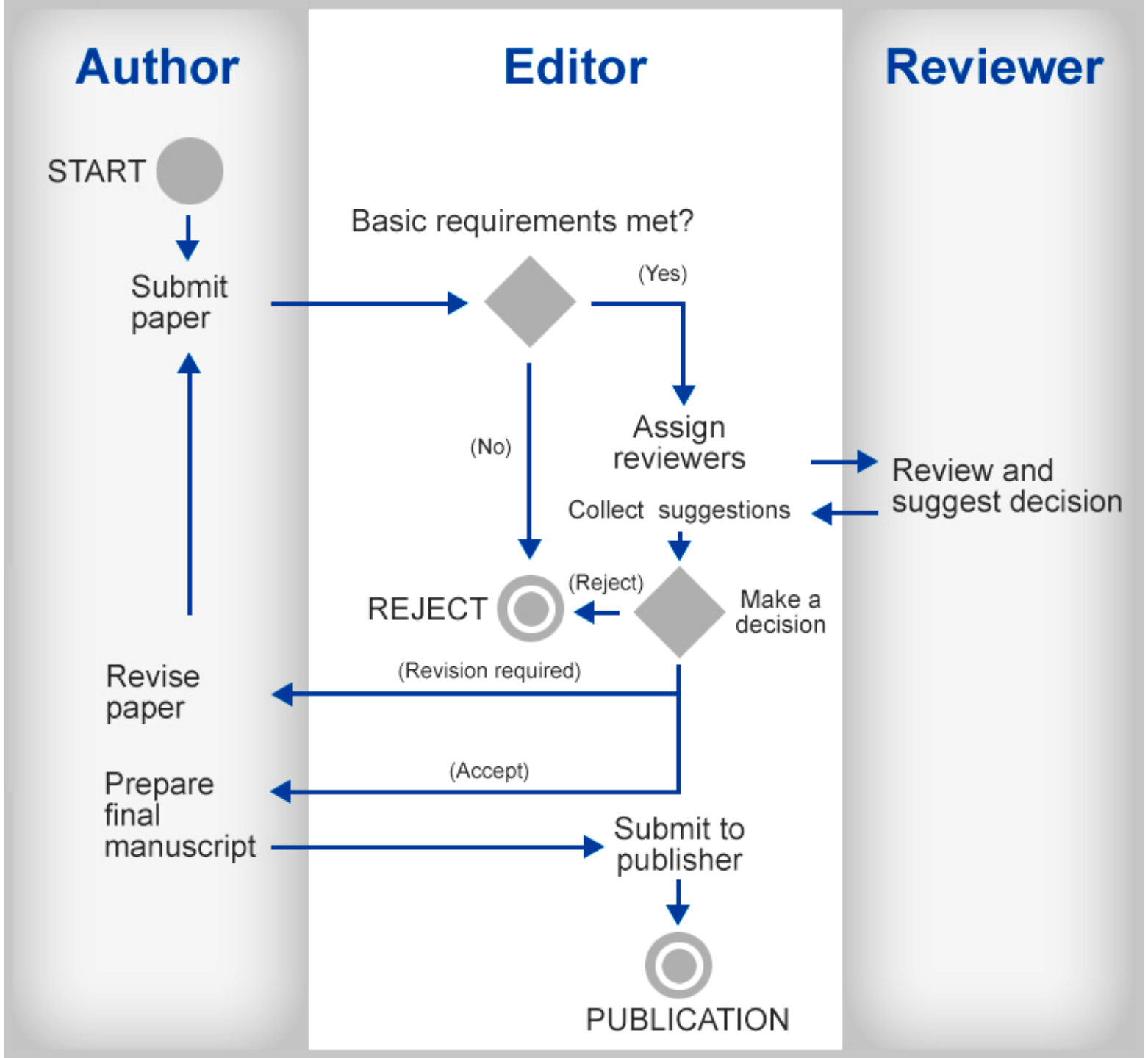
Author
Editor
Reviewer
START
Submit paper
Basic requirements met?
(Yes)
(No)
Assign reviewers
Review and suggest decision
Collect suggestions
REJECT
(Reject)
Make a decision
Revise paper
(Revision required)
Prepare final manuscript
(Accept)
Submit to publisher
PUBLICATION

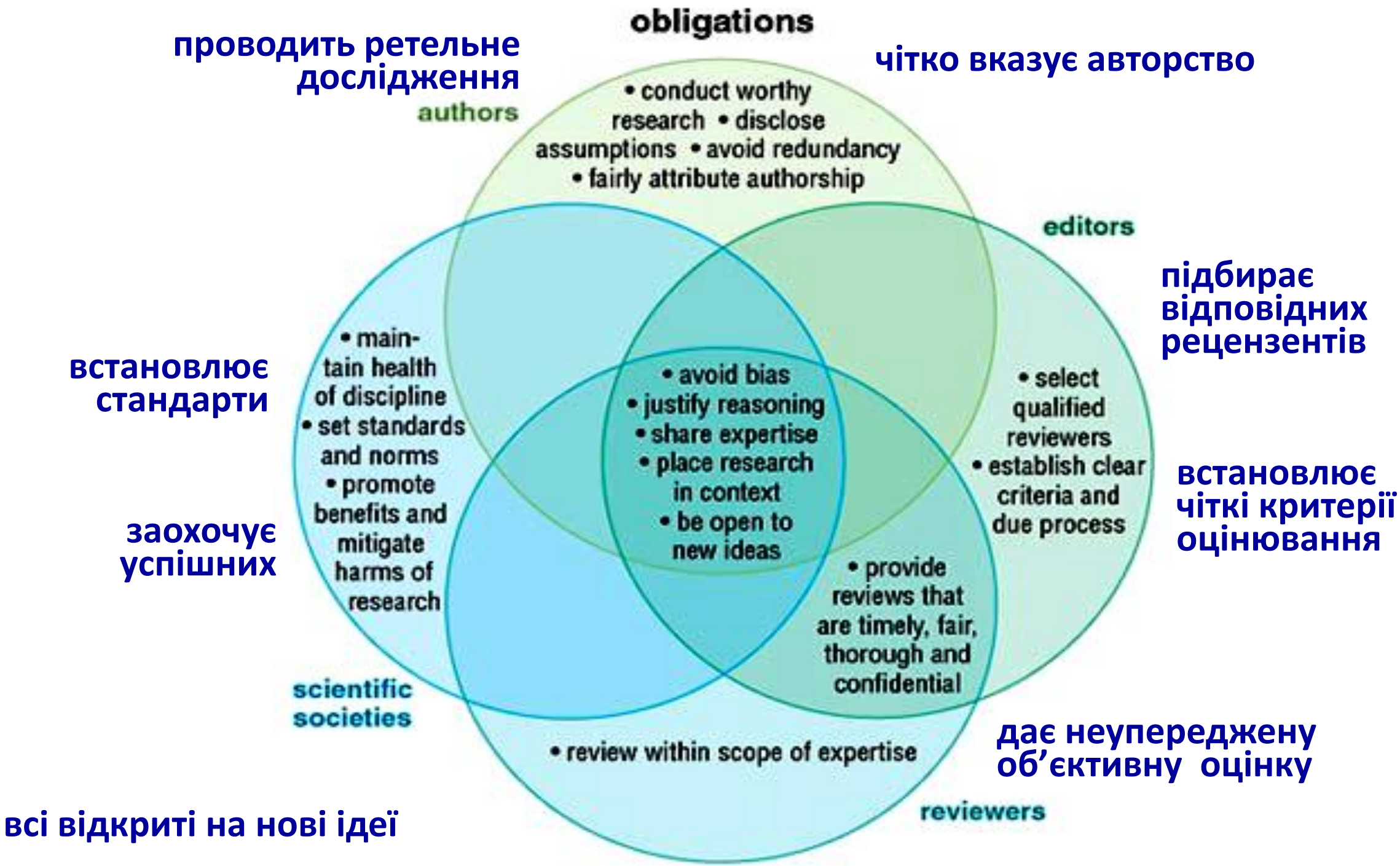
obligations
проводить ретельне дослідження
чітко вказує авторство
authors
• conduct worthy research • disclose assumptions • avoid redundancy • fairly attribute authorship
editors
підбирає відповідних рецензентів
встановлює стандарти
• main-tain health of discipline • set standards and norms • promote benefits and mitigate harms of research
• avoid bias • justify reasoning • share expertise • place research in context • be open to new ideas
• select qualified reviewers • establish clear criteria and due process
встановлює чіткі критерії оцінювання
заохочує успішних
• provide reviews that are timely, fair, thorough and confidential
scientific societies
дає неупереджену об’єктивну оцінку
• review within scope of expertise
reviewers
всі відкриті на нові ідеї

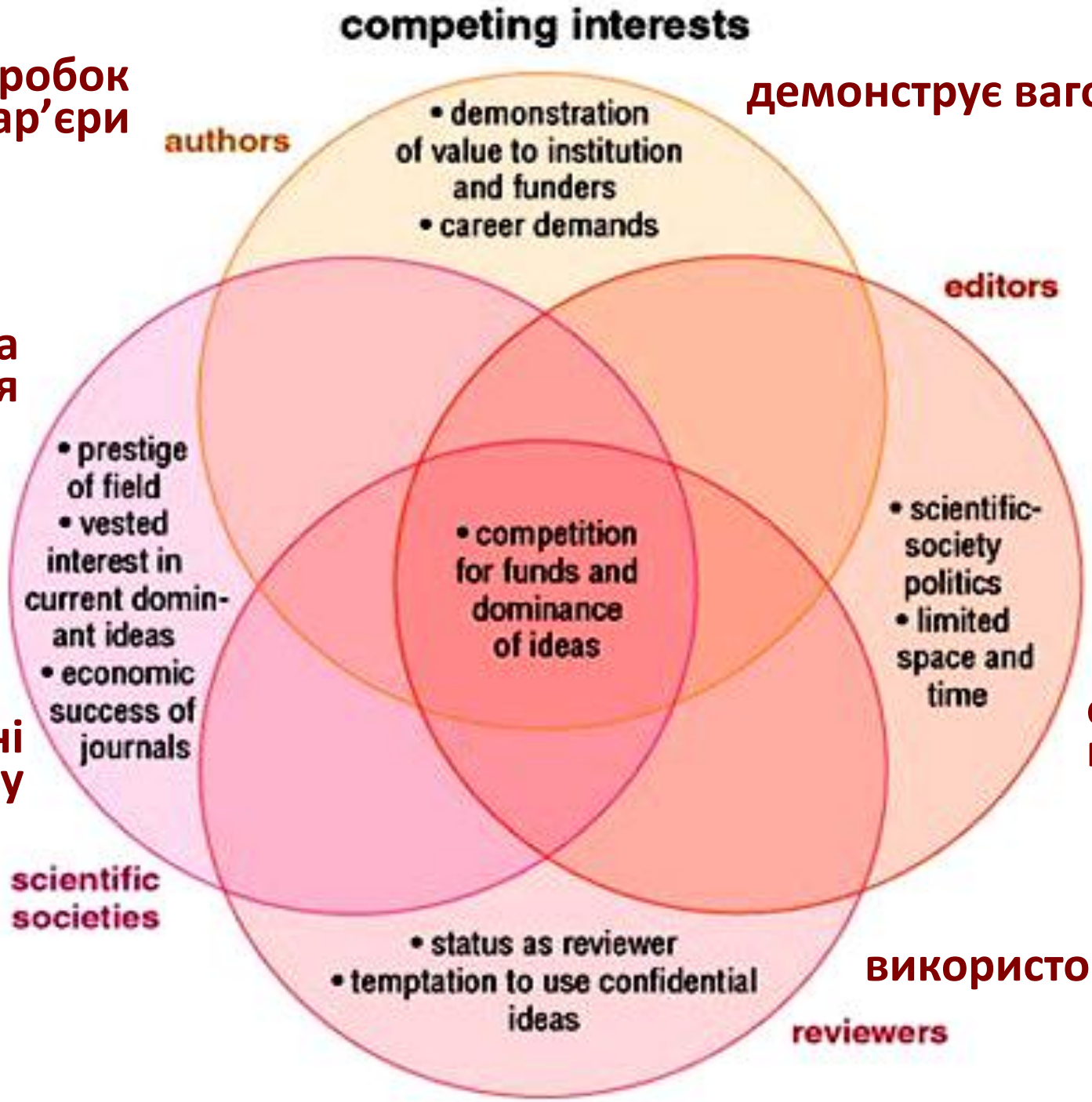

збирає доробок для кар'єри

демонструє вагомість інституту

конкуренція за фінансування

відображає політику наукового мікросоціуму

дбає про економічні показники журналу

обмеження по часу

використовує ідеї

PHYSICS AND CHEMISTRY OF SOLID STATE
V.21, No.2 (2020) pp. 338-346

Vasyl Stefanyk Precarpathian National University

DOI: 10.15330/pcss.21.2.338-346

ФІЗИКА І ХІМІЯ ТВЕРДОГО ТІЛА
Т. 21, № 2 (2020) С. 338-346

UDC 549.67

ISSN 1729-4428

N.V. Danyliuk, T.R. Tatarchuk, A.V. Shyichuk

Batch Microreactor for Photocatalytic Reactions Monitoring

Vasyl Stefanyk Precarpathian National University, Ivano-Frankivsk, Ukraine, danyliuk.nazariy@gmail.com

Photocatalytic oxidation of organic contaminants is a hot topic in environmental research. However, an effective purification process needs an effective photoreactor. Typical light sources such as mercury and halogen lamps are replaced with more energy efficient Light Emitting Diodes. In the current work, a miniature photoreactor with low catalyst consumption was presented. The work of the micro-photoreactor is investigated using anatase and P25 industrial titania as model catalysts. The key element of the microreactor is replaceable UV-LED. The used 365 nm emission wavelength is optimal for the model pollutant Rhodamine B dye. The micro-photoreactor is able almost completely to mineralize the Rhodamine B dye.

Key words: micro-photoreactor, rhodamine B, photocatalyst, LED, photodegradation.

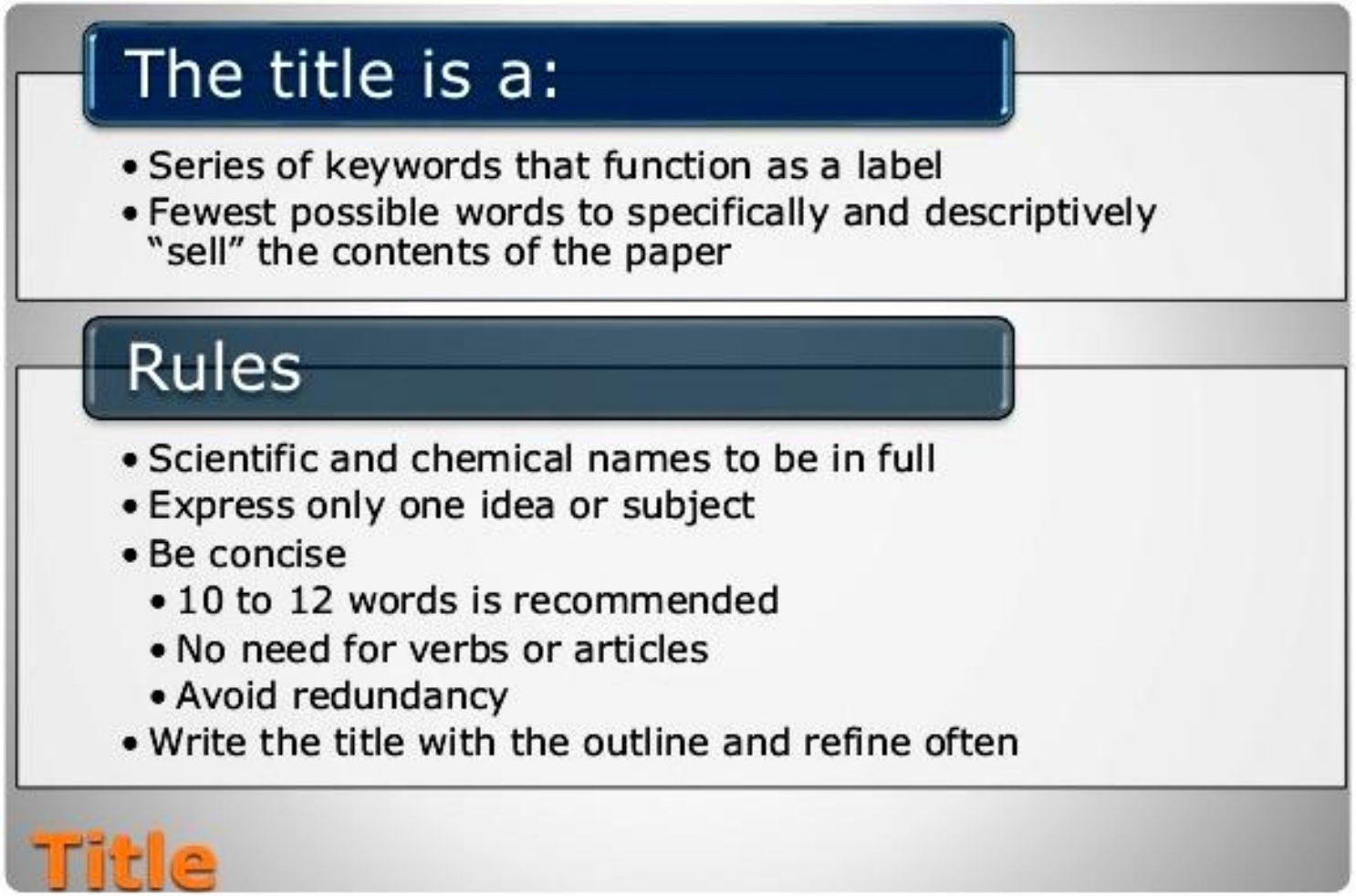

серія важливих слів

описує суть статі

уникати скорочень
тільки одна тема

чітко, стисло
відсутність дієслів

уникати надмірних деталей

Abstract

"From the mid-1970s through the mid-1980s, a network of young urban migrant men created an underground pulp fiction publishing industry in the city of Dar es Salaam. As texts that were produced in the underground economy of a city whose trajectory was increasingly charted outside of formalized planning and investment, these novellas reveal more than their narrative content alone. These texts were active components in the urban social worlds of the young men who produced them. They reveal a mode of urbanism otherwise obscured by narratives of decolonization, in which urban belonging was constituted less by national citizenship than by the construction of social networks, economic connections, and the crafting of reputations. This article argues that pulp fiction novellas of socialist era Dar es Salaam are artifacts of emergent forms of male sociability and mobility. In printing fictional stories about urban life on pilfered paper and ink, and distributing their texts through informal channels, these writers not only described urban communities, reputations, and networks, but also actually created them." (p. 210)

The first sentence introduces the **context** for this research and announces the **topic** under study.

The remaining sentences in this abstract interweave other essential information for an abstract for this article. The implied **research questions**: What do these texts mean? What is their historical and cultural significance, produced at this time, in this location, by these authors? The **argument** and the **significance** of this analysis in microcosm: these texts "reveal a mode or urbanism otherwise obscured . . ."; and "This article argues that pulp fiction novellas. . . ." This section also implies what **previous historical research** has obscured. And through the details in its argumentative claims, this section of the abstract implies the kinds of **methods** the author has used to interpret the novellas and the concepts under study (e.g., male sociability and mobility, urban communities, reputations, network. . .).

Abstract

"The growing economic resemblance of spouses has contributed to rising inequality by increasing the number of couples in which there are two high- or two low-earning partners. The dominant explanation for this trend is increased assortative mating. Previous research has primarily relied on cross-sectional data and thus has been unable to disentangle changes in assortative mating from changes in the division of spouses' paid labor—a potentially key mechanism given the dramatic rise in wives' labor supply. We use data from the Panel Study of Income Dynamics (PSID) to decompose the increase in the correlation between spouses' earnings and its contribution to inequality between 1970 and 2013 into parts due to (a) changes in assortative mating, and (b) changes in the division of paid labor. Contrary to what has often been assumed, the rise of economic homogamy and its contribution to inequality is largely attributable to changes in the division of paid labor rather than changes in sorting on earnings or earnings potential. Our findings indicate that the rise of economic homogamy cannot be explained by hypotheses centered on meeting and matching opportunities, and they show where in this process inequality is generated and where it is not." (p. 985)

The first sentence introduces the **topic** under study (the "economic resemblance of spouses"). This sentence also implies the **question** underlying this research study: what are the various causes—and the interrelationships among them—for this trend?

These next two sentences explain what **previous research** has demonstrated. By pointing out the limitations in the methods that were used in previous studies, they also provide a **rationale** for new research.

The data, research and analytical **methods** used in this new study.

The major **findings** from and **implications** and **significance** of this study.

Abstract

"Several studies have reported reprogramming of fibroblasts into induced cardiomyocytes; however, reprogramming into proliferative induced cardiac progenitor cells (iCPCs) remains to be accomplished. Here we report that a combination of 11 or 5 cardiac factors along with canonical Wnt and JAK/STAT signaling reprogrammed adult mouse cardiac, lung, and tail tip fibroblasts into iCPCs. The iCPCs were cardiac mesoderm-restricted progenitors that could be expanded extensively while maintaining multipo-tency to differentiate into cardiomyocytes, smooth muscle cells, and endothelial cells in vitro. Moreover, iCPCs injected into the cardiac crescent of mouse embryos differentiated into cardiomyocytes. iCPCs transplanted into the post-myocardial infarction mouse heart improved survival and differentiated into cardiomyocytes, smooth muscle cells, and endothelial cells. Lineage reprogramming of adult somatic cells into iCPCs provides a scalable cell source for drug discovery, disease modeling, and cardiac regenerative therapy." (p. 354)

The first sentence announces the **topic** under study, summarizes what's **already known** or been accomplished in **previous research**, and signals the **rationale and goals are for the new research and the problem** that the new research solves: How can researchers reprogram fibroblasts into iCPCs?

The **methods** the researchers developed to achieve their goal and a description of the **results**.

The **significance** or **implications**—for drug discovery, disease modeling, and therapy—of this reprogramming of adult somatic cells into iCPCs.

обов‘язкові розділи в науковій статті:

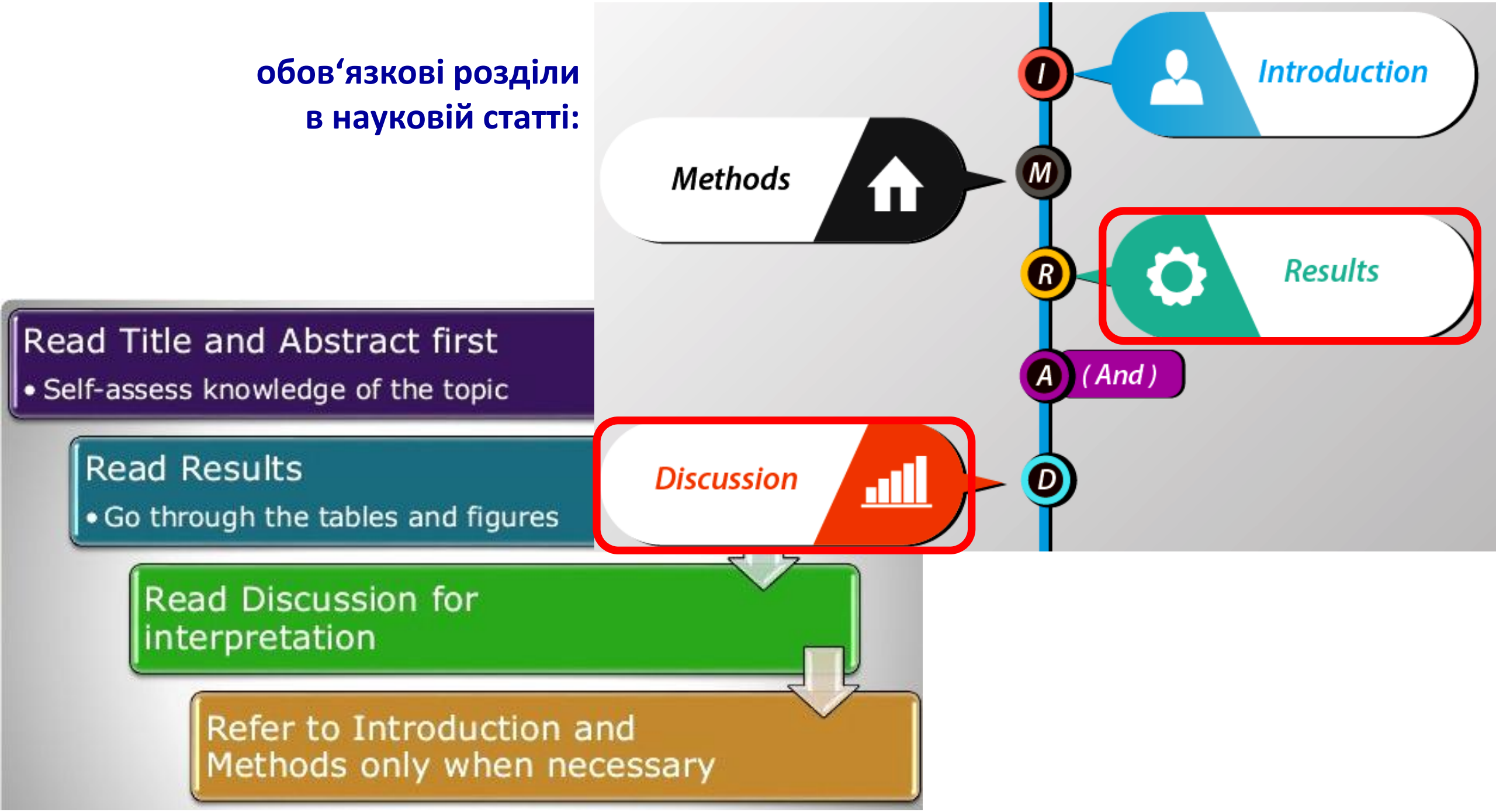

Introduction

In the last years, much attention is paid to "green" methods of wastewater remediation [1-4]. Photocatalysis is considered as a promising method of organic pollutant degradation. Photocatalytic oxidation leads to complete degradation of organic pollutants. The final products are non-toxic substances CO_2 and H_2O. Sunlight-activated photocatalyst leads to splitting of water molecules and formation of hydroxyl radicals. The highly aggressive radicals destroy the pollutant molecules [5-7]. It is known that the most active photocatalysts are TiO_2 [8-10] and ZnO [11,12]. Both the substances are inexpensive, non-toxic and chemically stable. However, the drawback is that these oxides absorb ultraviolet photons only. The UV part of the Sun energy is known to be 5 % only. For that reason, the key characteristics of photocatalyst is energy band gap, related strongly with crystalline structure. For example, the band gap for anatase, rutile, and brookite polymorphs of TiO_2 are 3.23 eV, 3.1 eV and 3.4 eV, respectively [13]. This is due to the difference in crystal lattice parameters and spatial locations of TiO_6 octahedra, in which Ti^{4+} ions are polymorph has an orthorhombic crystalline structure with lattice parameters a = 5.43 Å, b = 9.16 Å, and c = 5.13 Å [13]. The differences in crystalline structure cause different photocatalytic activities of the three titania polymorphs. The most active is rutile [14]. This is why extensive research are focused on simple and environment friendly methods of rutile production [15-19].

Titania photocatalytic activity may be improved via doping with heavy elements such as Fe, Co, Ga, W, Bi, Mo, V and Ni [20]. The dopants reduce rate of electron-holes recombination and extend the photocatalyst lifetime. Dopant amount should be chosen correctly. Too high modifier amount may distort crystal lattice and reduce photocatalytic activity. Optimal dopant amount is below 3 % [20]. On the other hand, heavy metal dopants are hazardous pollutants. Thus gradual photocatalyst destruction can lead to heavy metal dissemination. Surface properties of titania may be modified via grafting phosphate [21], arsenate [22], and carbonate [23] groups.

An important step in developing water purification method is optimization of experimental conditions. The photocatalyst efficiency is usually evaluated measuring

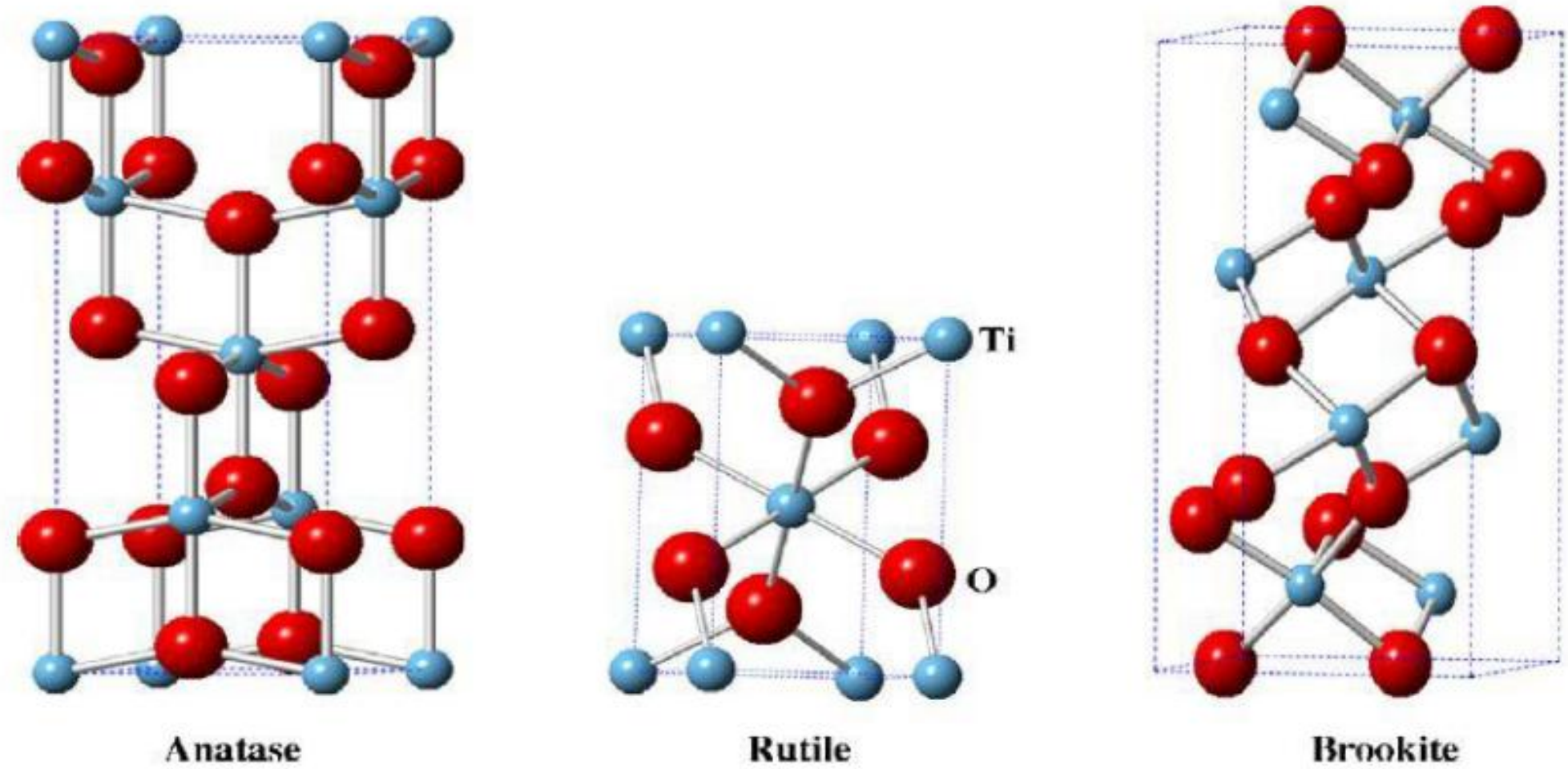

Fig. 1. Crystal structure of anatase, rutile and brookite [10].

easily monitored by photometry. The main factors affecting the rate and degree of RhB photodegradation are UV radiation power and photocatalyst activity. al. [6] described effect of H_2O_2 on RhB decomposition. Addition of H_2O_2 results in formation of large amount of hydroxyl radicals that destroy RhB molecules. However,

Table 1

Features of laboratory photocatalytic reactors

Reactor and solution volume	Model pollutant	Light source	Catalyst	Ref.
Photoreactor, 250 ml	textile dyes	UV-LED 11 mW, 200 mW (λ_{max} = 385 nm)	TiO_2	[35]
LED photoreactor, 1.5 L	$[Co(CN)_6]^{3-}$	UV-LED 30 W (λ_{max} = 365 nm)	TiO_2 (P25, Aeroxide)	[41]
Multistage rotating mesh support photoreactor	p-nitrophenol	11W UV-C lamps (λ_{max} = 253.7 nm)	TiO_2 P-25	[42]
Batch photocatalytic reactor	phenol	LED (20 mA - 25 mA) (λ_{max} = 375 nm)	Degussa P-25	[43]
Mini-photoreactor, 23 ml	n-decane	9 UVA LEDs 270 mW (λ_{max} = 365 nm)	TiO_2 - P25	[44]
Batch monolith photoreactor	CO_2 reduction with H_2	200W Hg (λ_{max} = 252 nm)	TiO_2 monolithic catalyst	[45]
Photo-microfluidic chip reactor, 0.0095 ml	propene oxidation	UV-LED light (0.55 W/cm^2)	TiO_2	[36]
UV-LEDs floating-bed photoreactor, 200 ml	caffeine, paracetamol	LED 14 W*m^{-1} (λ_{max} = 365 nm)	ZnO- Polystyrene	[11]
Continuous photoreactor, 1500 ml	Direct Red 23	LED 3.6 W	UV-LED/$S_2O_8^{2-}$	[26]

photoreactors are miniaturized in line with the basic principles of green chemistry. To be energy efficient, LED light sources should be optimized in terms of both power and emission spectrum. In the work [33] a LED-driven reactor with variable light intensity was presented. The surfactant sodium dodecylbenzenesulfonate (SDBS) was used as a model solution. The most effective removal (approximately 94 %) was observed with electric power consumption of 27.5 $mW \cdot cm^{-2}$. In terms of energy efficiency, the best result has been obtained with energy consumption of 3.22 $mW \cdot cm^{-2}$ and SDBS degradation of 90 %. Removal of SDBS was far less effective under mercury lamp illumination. With degradation of RhB dye, energy consumption was several times higher than that with using modernized LED reactor. These data suggest that mercury lamps should be replaced by LEDs. Bukman et al. [34] proposed a new approach to evaluation of photoreaction performance. UV LED was combined with a

I. Experimental

Mixed anatase-rutile titania P25 come from Degussa (Germany). Reagent-grade titanium dioxide (anatase 99.7 %) and Rhodamine B dye ($C_{28}H_{31}ClN_2O_3$) were obtained from Sigma (now Merck). Structural formula of the Rhodamine B dye is presented in Fig. 2.

Spectra in the range 350 - 700 nm were registered with spectrophotometer ULAB 102-UV using 5 mm quartz cuvettes. Calibration line was plotted using absorbance at 558 nm against RhB concentration in the range from 1 to 20 mg/L. The calibration plot is quite straight line with determination coefficient $R^2 = 0.999$ (Fig. 3-b).

Photodegradation experiments were carried out using 30 mL of 5 mg/L aqueous solution of the RhB dye and 30 mg of titania photocatalyst. Before the experiment, the reaction solution was stirred for 30 min in order to

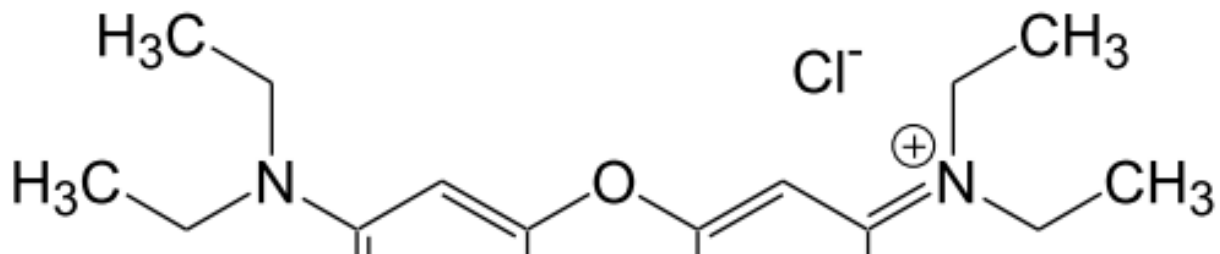

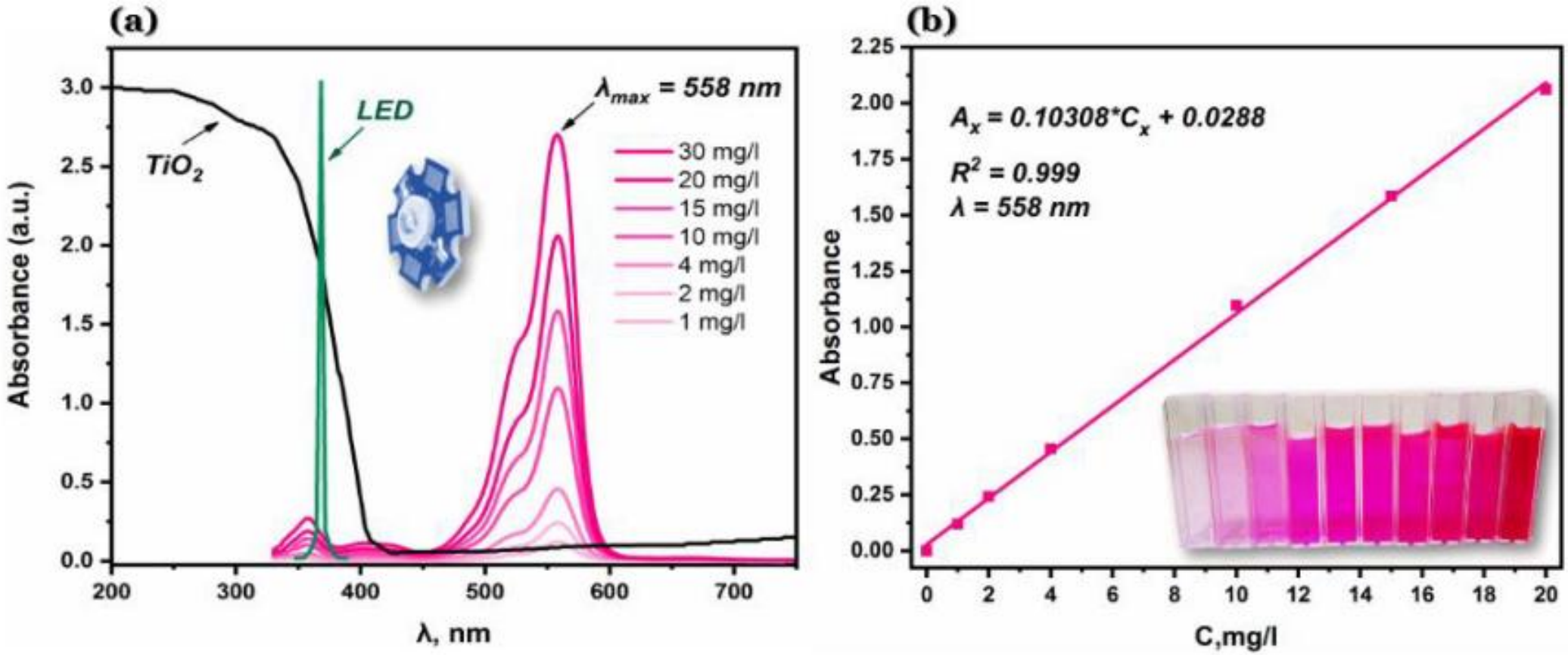

Fig. 3. (a) UV-vis spectrum of RhB solutions at indicated concentrations. (b) Absorbance at 558 nm (the spectral peak wavelength) versus RhB concentration.

equilibrate adsorption of the dye on titania surface. The solution pH was in the range from 6 to 7. Samples were collected at 0, 180, and 300 minutes. Fig. 4 shows images of RhB solution before and after photo-degradation. The sample of 5 mL was centrifuged for 5

Fig. 6. The cuvette holder is moved to collect samples of the solution.

3.2. Photocatalytic experiments.

The microreactor was designed for rapid testing of photocatalysts. The exemplary study presents

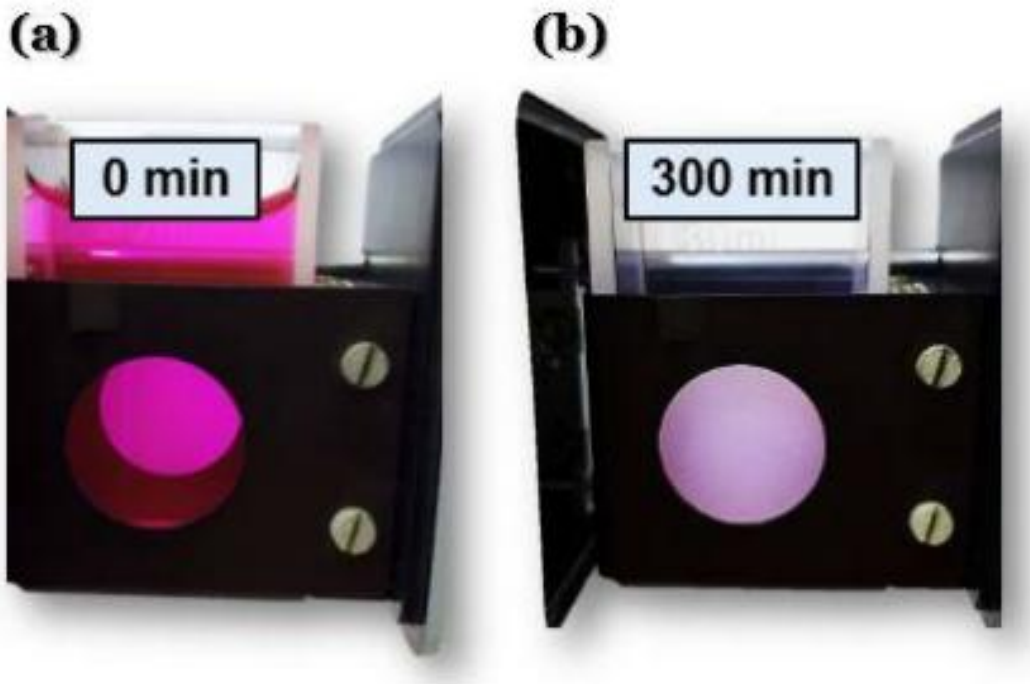

Fig. 4. Images of RhB solution before (a) and after (b) photo-degradation.

II. Results

3.1. Design of the micro-photoreactor.

Principal scheme of the micro-photoreactor is presented in Fig. 5. The main element is rectangle glass cuvette with 20 mm optical path. The cuvette volume is 30 mL. Magnetic stirrer ensures even distribution of photocatalyst. The light source is a LED supplied with 700 mA current at 3.4 - 3.8 V. The power LED is placed

Replaceable light source allows to choose wavelength optimal to absorbance spectrum of the substance studied. If the goal of a study is stability test of a substance, the wave length should match peak of the substance absorption spectrum. On contrary, a study on a catalyst efficiency requires minimal light absorption by a model substance. In the present study, wave length of the LED light source was 365 nm. This wavelength corresponds to the range of minimal light absorption of the RhB dye (Fig. 3a). Thus, photodegradation of RhB dye is minimalized. On the other hand, the LED emission spectrum corresponds to the absorption range of the titania photocatalyst used (Fig. 3a). The TiO_2 photocatalyst is usually activated with irradiation of short wavelengths less than 400 nm. Optical power of the light source should be optimal for a studied catalyst [58]. In the present study, the luminous power was 15 lumen.

Efficiencies of the studied photocatalyts were evaluated using extent of the dye degradation. The numerical data are presented in Table 3. The data indicate clearly that the P25 catalyst has higher activity than anatase.

Spectra of the degraded RhB samples are presented in Fig. 7. There was no new spectral band registered.

Table 3

Extent of RhB dye degradation using P25 and anatase photocatalysts

Catalyst	Degradation (%)	
	180 min	300 min
P25	67.5	97.3
anatase	39.7	59.6

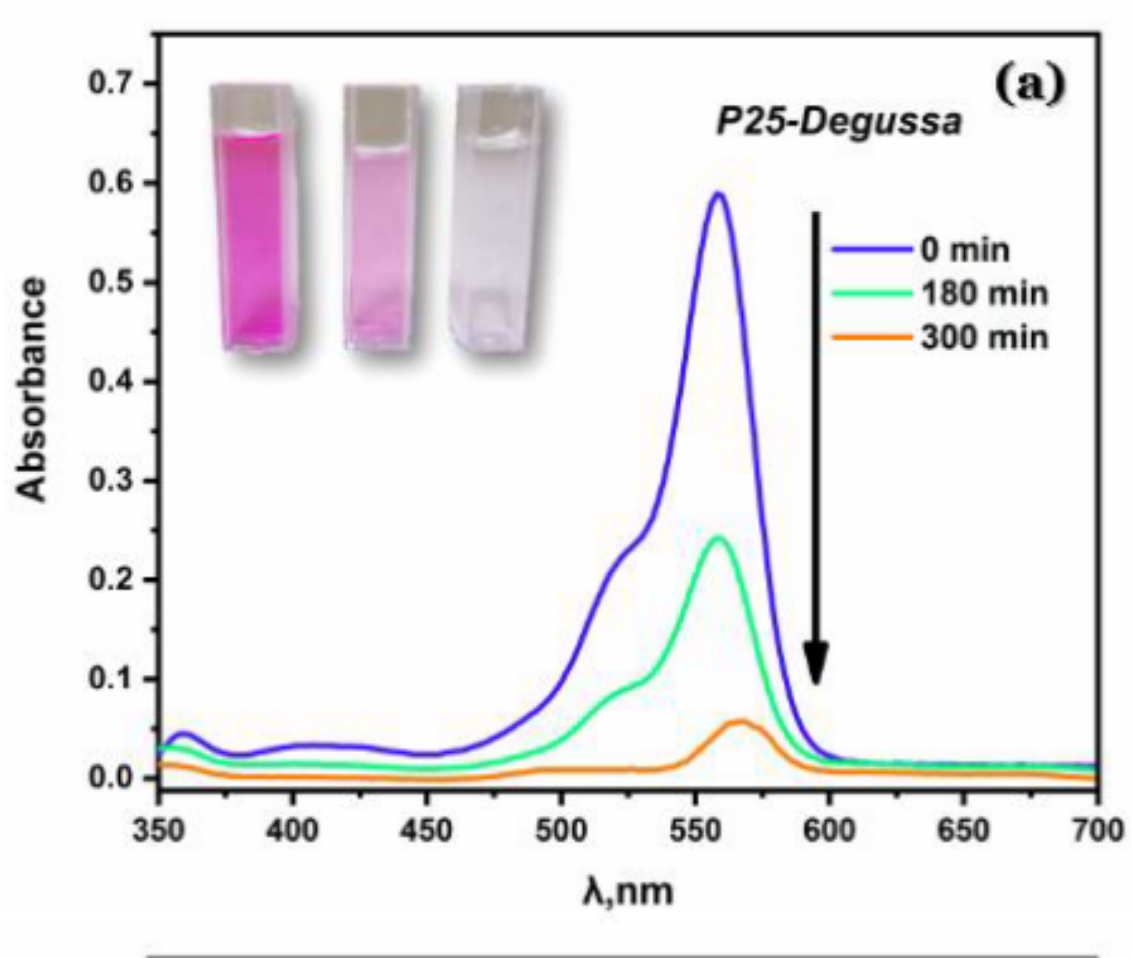

markedly to shorter wavelength (Fig. 7b). In the case of the P25 catalyst, spectra of the samples are slightly shifted to longer wavelengths (Fig. 7a). Probable mechanism of RhB photodegradation comprises three stages [6, 57]. At first, auxochrome ethyl groups are detached from amino groups. Second, the deethylated products lose carboxyle group. Third stage is decomposition of chromophore core and formation of low molecular acidic compounds. Finally, carbon dioxide and water are formed.

The comparison of photocatalytic micro-reactors aimed to degradation of dyes are presented in Table 4. The advantages of the presented micro-reactor are low operating costs, simple experimental design, high energy efficiency and very narrow emission spectrum.

Conclusions

LED photocatalytic reactors can be successfully used to study degradation of organic pollutants. The important features of the LED UV sources are the following: (i) high energy efficiency; (ii) small size and low toxicity (Hg-free); (iii) high durability leading to long service

[1] I. Anastopoulos, I. Pashalidis, A.G. Orfanos, I.D. Manariotis, T. Tatarchuk, L. Sellaoui, A. Bonilla-Petriciolet, A. Mittal, A. Núñez-Delgado, J. Environ. Manage. 261 (2020) (https://doi.org/10.1016/j.jenvman.2020.110236).
[2] M. Naushad, A.A. Alqadami, A.A. Al-Kahtani, T. Ahamad, M.R. Awual, T. Tatarchuk, J. Mol. Liq. 296. 112075 (2019) (https://doi.org/10.1016/J.MOLLIQ.2019.112075).
[3] T. Tatarchuk, A. Shyichuk, I. Mironyuk, M. Naushad, J. Mol. Liq. 293, 111563 (2019) (https://doi.org/10.1016/j.molliq.2019.111563).
[4] M. Naushad, Z.A. ALOthman, Desalin. Water Treat. 53, 2158 (2015) (https://doi.org/10.1080/19443994.2013.862744).
[5] N. Phutanon, P. Pisitsak, H. Manuspiya, S. Ummartyotin, J. Sci. Adv. Mater. Devices. 3, 310 (2018) (https://doi.org/10.1016/j.jsamd.2018.05.001).
[6] N. Guo, H. Liu, Y. Fu, J. Hu, Optik (Stuttg) 201, 163537 (2019) (https://doi.org/10.1016/j.ijleo.2019.163537).
[7] Y. Wang, Q. Yang, X. Wang, J. Yang, Y. Dai, Y. He, W. Chen, W. Zhang, Mater. Sci. Eng. B Solid-State Mater. Adv. Technol. 244, 12 (2019) (https://doi.org/10.1016/j.mseb.2019.04.005).
[8] M.A. Lazar, S. Varghese, S.S. Nair, Catalysts 2, 572 (2012) (https://doi.org/10.3390/catal2040572).
[9] K. Karthik, S. Vijayalakshmi, A. Phuruangrat, V. Revathi, U. Verma, J. Clust. Sci. 30 (2019) (https://doi.org/10.1007/s10876-019-01556-1).
[10] R. Aswini, S. Murugesan, K. Kannan, Int. J. Environ. Anal. Chem. 00 (2020) (https://doi.org/10.1080/03067319.2020.1718668).
[11] V. Vaiano, M. Matarangolo, O. Sacco, Chem. Eng. J. 350, 703 (2018) (https://doi.org/10.1016/j.cej.2018.06.011).
[12] S. Sa-nguanprang, A. Phuruangrat, K. Karthik, S. Thongtem, T. Thongtem, J. Aust. Ceram. Soc. (2020) (https://doi.org/10.1007/s41779-019-00447-y).

Review Article

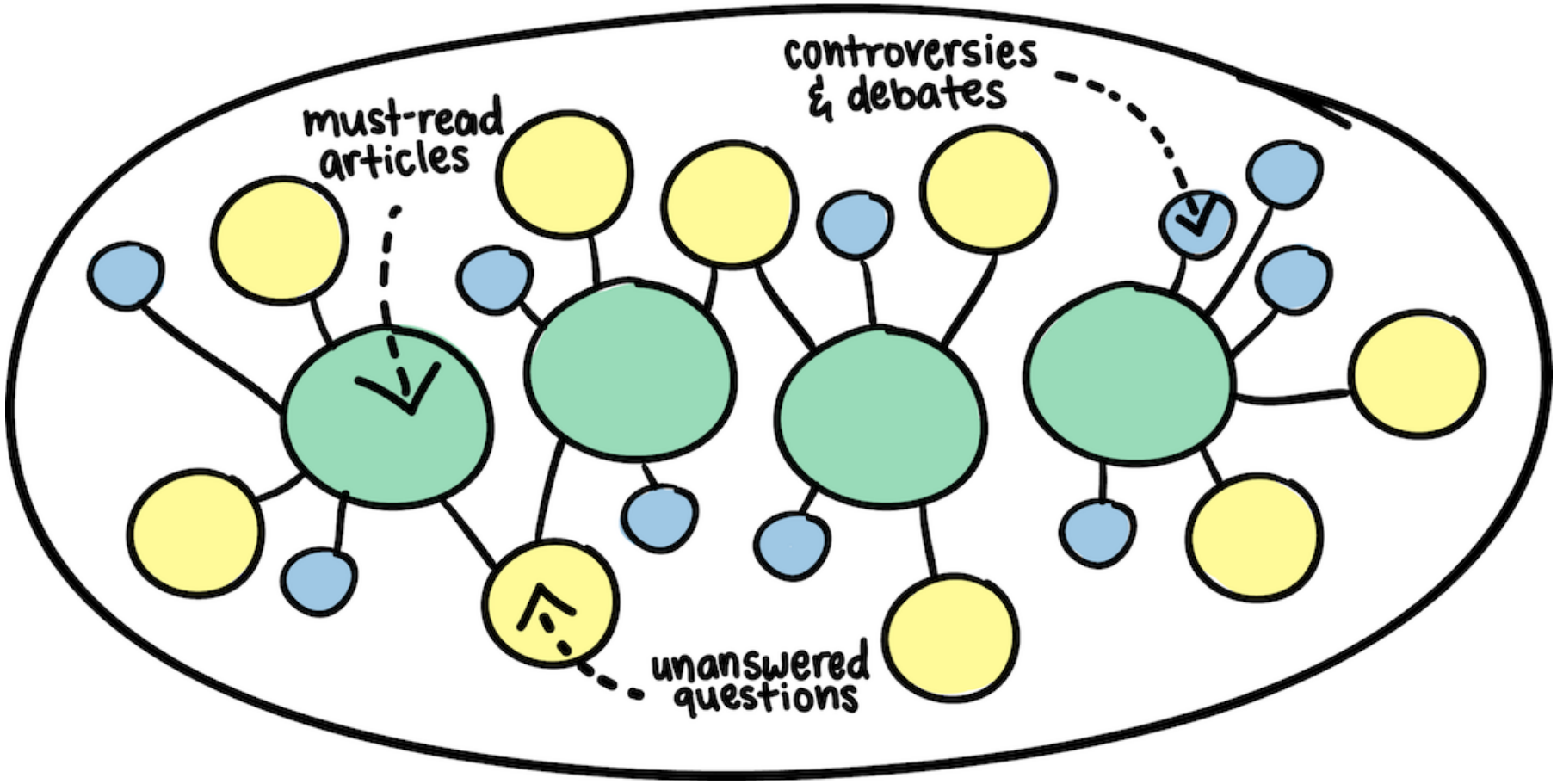

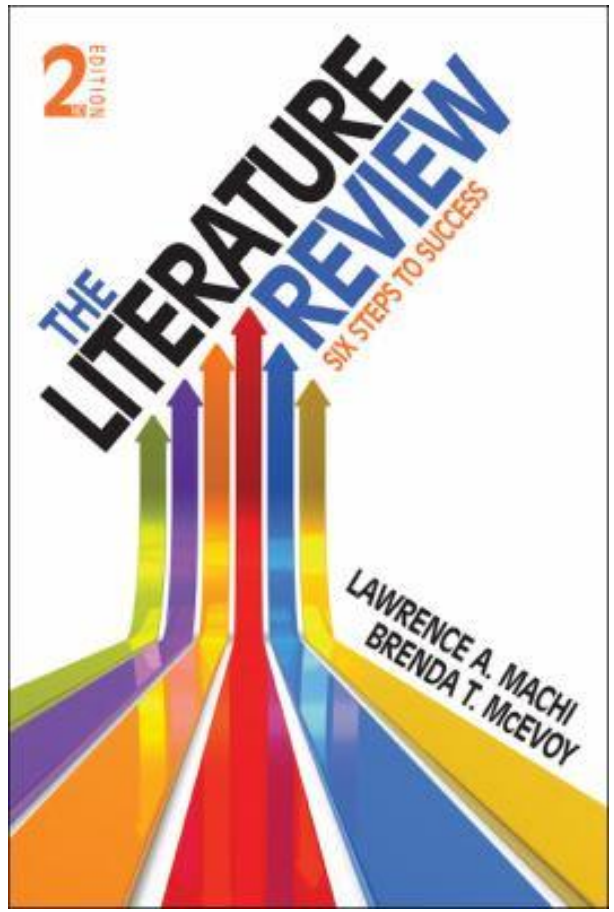

Journal of Molecular Liquids 309 (2020) 113077

Contents lists available at ScienceDirect

Journal of Molecular Liquids

journal homepage: www.elsevier.com/locate/molliq

Review

Halloysite nanotubes and halloysite-based composites for environmental and biomedical applications

Nazarii Danyliuk [a], Jolanta Tomaszewska [b], Tetiana Tatarchuk [c,*]

[a] Educational and Scientific Center of Material Science and Nanotechnology, Vasyl Stefanyk Precarpathian National University, Ivano-Frankivsk 76018, Ukraine
[b] Faculty of Chemical Technology and Engineering, UTP University of Science and Technology, 3 Seminaryjna Street, 85-326 Bydgoszcz, Poland
[c] Department of Chemistry, Vasyl Stefanyk Precarpathian National University, 57 Shevchenko Street, 76018 Ivano-Frankivsk, Ukraine

ARTICLE INFO

Article history:
Received 22 February 2020
Received in revised form 29 March 2020
Accepted 3 April 2020

ABSTRACT

Halloysite is a natural tubular mineral with unique properties. It can be used in a various fields of industries. The aim of current review is to describe the structural properties and methods of halloysite surface modification, what led to the extension of its application. The achievements of scientists over the last 10 years indicate that halloysite is a promising material for drug delivery, as polymer filler, as matrix for photocatalysts and adsorbents

ture prospects for halloysite composites using have been identified. This review provides the latest findings from researchers, which sheds light on future halloysite studies.

Contents

1. Introduction

Chemical compounds in the tubes form have attracted an interest of scientists due to their possibilities to demonstrate a wide range of properties [1,2]. The nanotubes may originate from nature (natural aluminosilicate nanotubes – halloysite) and may be obtained through synthetic way [3,4]. The layered structure of these minerals consists of tetrahedral Si-O and octahedral Al-O sheets, which are linked into a single layer [5]. The halloysite occurs also in spheroidal, flat and other forms. In the nature, the aluminosilicate nanotubes were formed

* Corresponding author

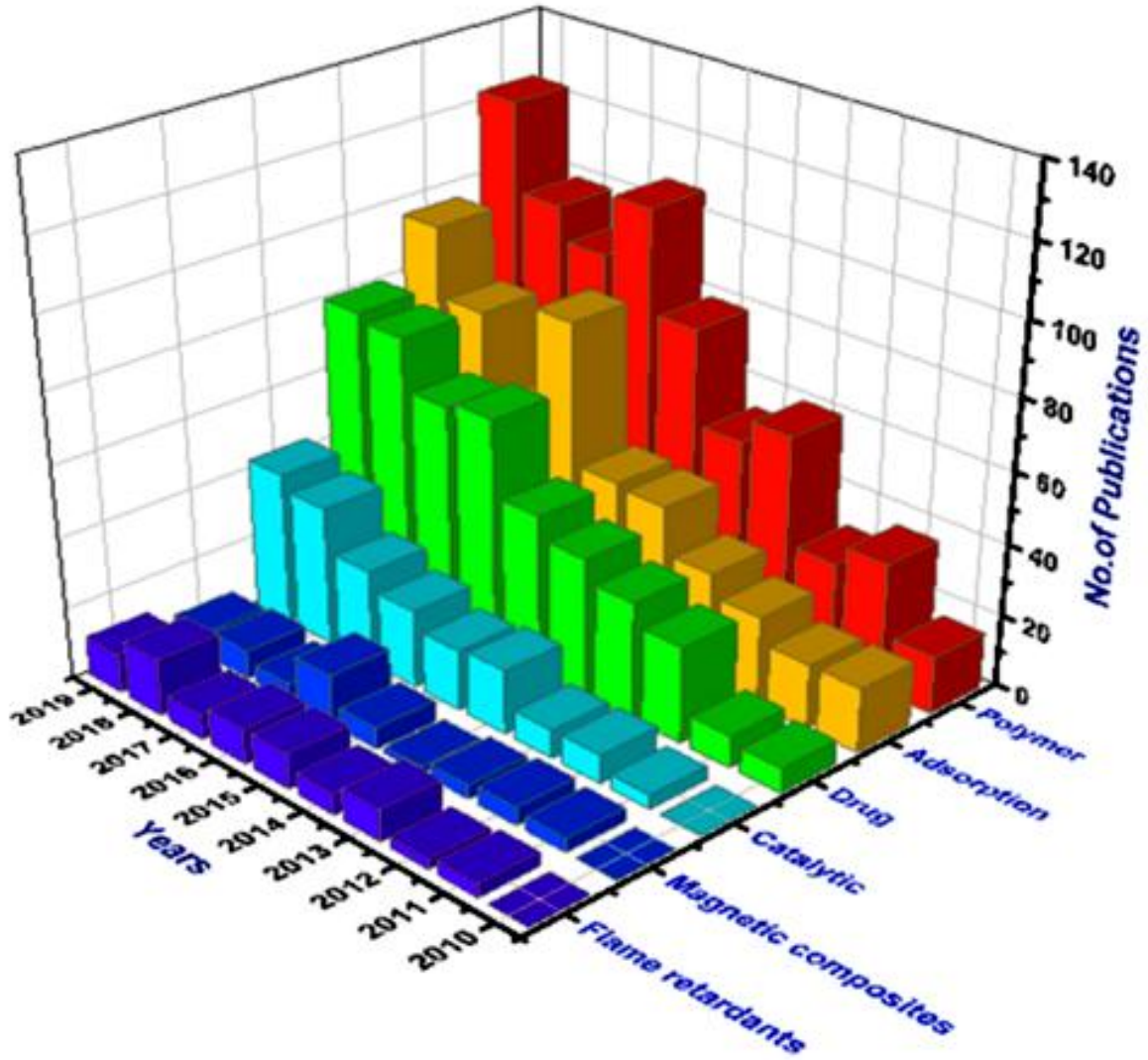

Fig. 1. The number of scientific publications based on the HNTs investigations over the last 10 years.
(The data obtained from Scopus database on February 2020.)

of halloysite and kaolinite made their interlayer spaces suitable also for the intercalation of herbicide amitrole (AMT) [4].

3. Applications of halloysite and halloysite-based composites

3.1. Adsorption properties of halloysite and its composites

One of the most important task for environmental application is the modification of natural and synthetic porous materials in order to get the adsorbents for pollutants removal from aquatic environment [46–48]. The halloysite nanotubes are among promising adsorbents due to the surface of nanotube cavities, which are involved in adsorption processes [49]. HNTs exhibit less adsorption capacity compared to other adsorbents, so the solution is to modify the halloysite surface [50]. Nowadays, many publications related to the HNTs modification have been published [16–23]. The HNTs surface can be modified in order to adsorb the chloroanilines [21], ciprofloxacin [19], benzene [20], heavy metal ions [16], iodates [17], CO_2 [18], arsenic compounds [23], for simultaneous adsorption of Cr (VI) and Sb (V) [22].

Deng et al. [20] conducted the acidic treatment of HNTs surface in order to improve its adsorption properties and investigate the benzene adsorption. Annealing at 800 °C resulted in the dehydroxylation and phase separation of amorphous SiO_2 and Al_2O_3. Due to the dehydroxylation, the hydrophilicity of halloysite is reduced, which leads to the affinity of hydrophobic benzene molecules. The adsorption capacity of

ical precipitation route. The transmission electron microscopy shows that the Fe_3O_4 nanoparticles with a diameter of 3–5 nm were deposited on the HNTs surface and exhibit magnetic property (Ms = 8.47 emu/g), which makes it easy to separate it from the aqueous solution (Fig. 12). The HNTs-Fe_3O_4 nanocomposite showed excellent adsorption capacity with respect to the methyl violet dye – 90,09 mg/g. The calcination was proposed as a method for adsorbent reuse.

contaminated water due to the external magnetic field applying.

Wan et al. [73] synthesized the core@double-shell structured HNTs/Fe_3O_4/poly(DA + KH550) magnetic composite for effective removal of methylene blue from an aqueous solution. The obtained adsorbent consists of a halloysite core and two layers with active adsorption sites: the magnetic layer (necessary for magnetic separation) and the second layer of polydopamine and KH550 as silane coupling agent. The

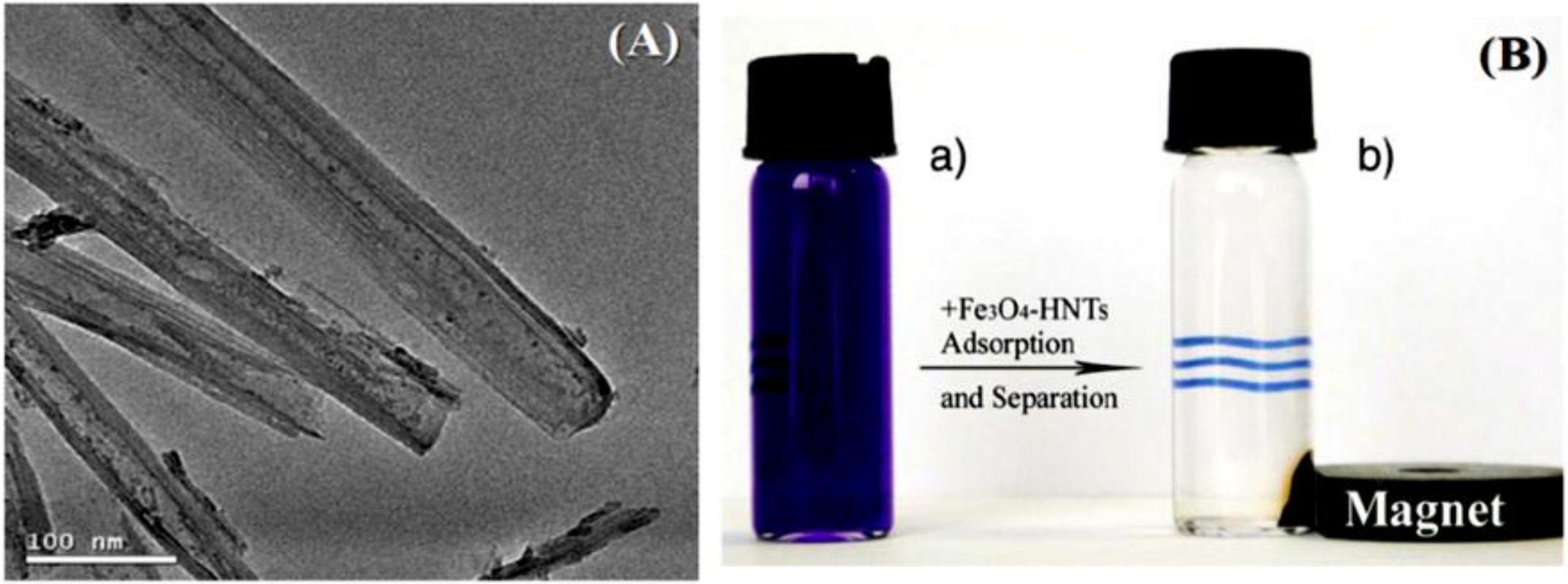

Fig. 12. TEM micrographs for Fe_3O_4–HNTs (A), separation of Fe_3O_4–HNTs from solution by a magnet, (a) MV solution, (b) magnetic separation after adsorption onto Fe_3O_4–HNTs. (Reprinted from [70], Copyright (2012), with permission from Elsevier.)

temperatures, what makes it as promising bioactive component for bone tissue regeneration.

Suner et al. [78] presented biocompatible cryogel composites based on hyaluronic acid (HA) and HNTs for use in tissue engineering. Cryogel composites of HA/HNTs were prepared in different ratios of HA:HNTs, for example, 1:0; 1:0.5; 1:1 and 1:2 in cryogenic conditions in order to obtain macroporous nanosystems with pore sizes from 50 μm to 500 μm. It is revealed that rooting of HNTs in HA influences the Young's modulus. For example, the ratio of HA:HNTs = 1:2 leds to increase of Young's modulus in 2.5 times (from 38 ± 1 to 99 ± 4 kPa). Also cryogels based on HA:HNTs composite in ratio as 1:2 showed high biocompatibility with blood with a hemolysis coefficient of 1.37 ± 0.11% and thrombogenic activity with a blood clotting index of 17.3 ± 4.8. In addition, HA:HNTs cryogel composites have shown excellent results in the study of proliferation of rat mesenchymal stem cells (MSCs) and human colon cancer cells (HCT116). Based on the obtained results, it can be stated that the prepared cryogel composites HA:HNTs are promising materials for tissue engineering with macroporous structure and good compatibility with blood. Such composites can find many applications in the biomedical field to promote cell viability and regeneration.

4. Conclusions

Halloysite is safe and environmentally friendly nanomaterial available in large amounts and may be used for large-scale industrial applica-

Acknowledgements

The work was carried out within the framework of the project number MESU 0118U000258, supported by the Ministry of Education and Science of Ukraine.

References

[1] S. Saadat, G. Pandey, M. Tharmavaram, V. Braganza, D. Rawtani, Nano-interfacial decoration of halloysite nanotubes for the development of antimicrobial nanocomposites, Adv. Colloid Interf. Sci. 275 (2020), 102063. https://doi.org/10.1016/J.CIS.2019.102063.

[2] A. Kassem, G.M. Ayoub, L. Malaeb, Antibacterial activity of chitosan nanocomposites and carbon nanotubes: a review, Sci. Total Environ. 668 (2019) 566–576, https://doi.org/10.1016/J.SCITOTENV.2019.02.446.

[3] I. Anastopoulos, A. Mittal, M. Usman, J. Mittal, G. Yu, A. Núñez-Delgado, M. Kornaros, A review on halloysite-based adsorbents to remove pollutants in water and wastewater, J. Mol. Liq. 269 (2018) 855–868, https://doi.org/10.1016/j.molliq.2018.08.104.

[4] D. Tan, P. Yuan, F. Annabi-Bergaya, F. Dong, D. Liu, H. He, A comparative study of tubular halloysite and platy kaolinite as carriers for the loading and release of the herbicide amitrole, Appl. Clay Sci. 114 (2015) 190–196, https://doi.org/10.1016/j.clay.2015.05.024.

[5] Y. Lvov, W. Wang, L. Zhang, R. Fakhrullin, Halloysite clay nanotubes for loading and sustained release of functional compounds, Adv. Mater. 28 (2016) 1227–1250, https://doi.org/10.1002/adma.201502341.

[6] E.G. Bediako, E. Nyankson, D. Dodoo-Arhin, B. Agyei-Tuffour, D. Łukowiec, B. Tomiczek, A. Yaya, J.K. Efavi, Modified halloysite nanoclay as a vehicle for sustained drug delivery, Heliyon 4 (2018) https://doi.org/10.1016/j.heliyon.2018.e00689.

[7] C. Cheng, Y. Gao, W. Song, Q. Zhao, H. Zhang, H. Zhang, Halloysite nanotube-based H2O2-responsive drug delivery system with a turn on effect on fluorescence for real-time monitoring, Chem. Eng. J. 380 (2020), 122474. https://doi.org/10.1016/j.

[70] J. Duan, R. Liu, T. Chen, B. Zhang, J. Liu, Halloysite nanotube-Fe3O4 composite for removal of methyl violet from aqueous solutions, Desalination 293 (2012) 46–52, https://doi.org/10.1016/j.desal.2012.02.022.
[71] X. Song, L. Zhou, Y. Zhang, P. Chen, Z. Yang, A novel cactus-like Fe3O4/halloysite nanocomposite for arsenite and arsenate removal from water, J. Clean. Prod. 224 (2019) 573–582, https://doi.org/10.1016/j.jclepro.2019.03.230.
[72] Y. Xie, D. Qian, D. Wu, X. Ma, Magnetic halloysite nanotubes/iron oxide composites for the adsorption of dyes, Chem. Eng. J. 168 (2011) 959–963, https://doi.org/10.1016/j.cej.2011.02.031.
[73] X. Wan, Y. Zhan, Z. Long, G. Zeng, Y. He, Core@double-shell structured magnetic halloysite nanotube nano-hybrid as efficient recyclable adsorbent for methylene blue removal, Chem. Eng. J. 330 (2017) 491–504, https://doi.org/10.1016/j.cej.2017.07.178.
[74] M.A. Bonifacio, P. Gentile, A.M. Ferreira, S. Cometa, E. De Giglio, Insight into halloysite nanotubes-loaded gellan gum hydrogels for soft tissue engineering applications, Carbohydr. Polym. 163 (2017) 280–291, https://doi.org/10.1016/j.carbpol.2017.01.064.
[75] Q. Chen, S. Liang, J. Wang, G.P. Simon, Manipulation of mechanical compliance of elastomeric PGS by incorporation of halloysite nanotubes for soft tissue engineering applications, J. Mech. Behav. Biomed. Mater. 4 (2011) 1805–1818, https://doi.org/10.1016/j.jmbbm.2011.05.038.
[76] G. Lazzara, G. Cavallaro, A. Panchal, R. Fakhrullin, A. Stavitskaya, V. Vinokurov, Y. Lvov, Current Opinion in Colloid & Interface Science An assembly of organic-inorganic composites using halloysite clay nanotubes, Curr. Opin. Colloid Interface Sci. 35 (2018) 42–50, https://doi.org/10.1016/j.cocis.2018.01.002.
[77] A. Pietraszek, A. Karewicz, M. Widnic, D. Lachowicz, M. Gajewska, A. Bernasik, M. Nowakowska, Halloysite-alkaline phosphatase system—a potential bioactive component of scaffold for bone tissue engineering, Colloids Surfaces B Biointerfaces 173 (2019) 1–8, https://doi.org/10.1016/j.colsurfb.2018.09.040.
[78] S.S. Suner, S. Demirci, B. Yetiskin, R. Fakhrullin, E. Naumenko, O. Okay, R.S. Ayyala, N. Sahiner, Cryogel composites based on hyaluronic acid and halloysite nanotubes as scaffold for tissue engineering, Int. J. Biol. Macromol. 130 (2019) 627–635, https://doi.org/10.1016/j.ijbiomac.2019.03.025.
[79] M. Tharmavaram, G. Pandey, D. Rawtani, Surface modified halloysite nanotubes: a flexible interface for biological, environmental and catalytic applications, Adv. Colloid Interf. Sci. 261 (2018) 82–101, https://doi.org/10.1016/j.cis.2018.09.001.

Evaluate which journal is right for your article

- Impact Factor
- Subject Specific Impact Factor (http://tinyurl.com/scopusimpact)
- SCImago Journal & Country Ranking (http://scimagojr.com/)
- Journal Analyzer
- *h*-Index of other authors
- Ask yourself "Where will my article have the greatest impact?"
- If possible, submit to a "niche" or special interest journal

Impact Factor (IF)

[the average annual number of citations per article published]

- For example, the 2013 impact factor for a journal would be calculated as follows:
  - *A* = the number of times articles published in 2011 and 2012 were cited in indexed journals during 2013
  - *B* = the number of "citable items" (usually articles, reviews, proceedings or notes; not editorials and letters-to-the-Editor) published in 2011 and 2012
  - 2013 impact factor = *A*/*B*
  - **e.g.** $\frac{\textbf{600 citations}}{\textbf{150 + 150 articles}} = \textbf{2}$

What does having impact factor mean?

кількість цитувань змінюється в часі

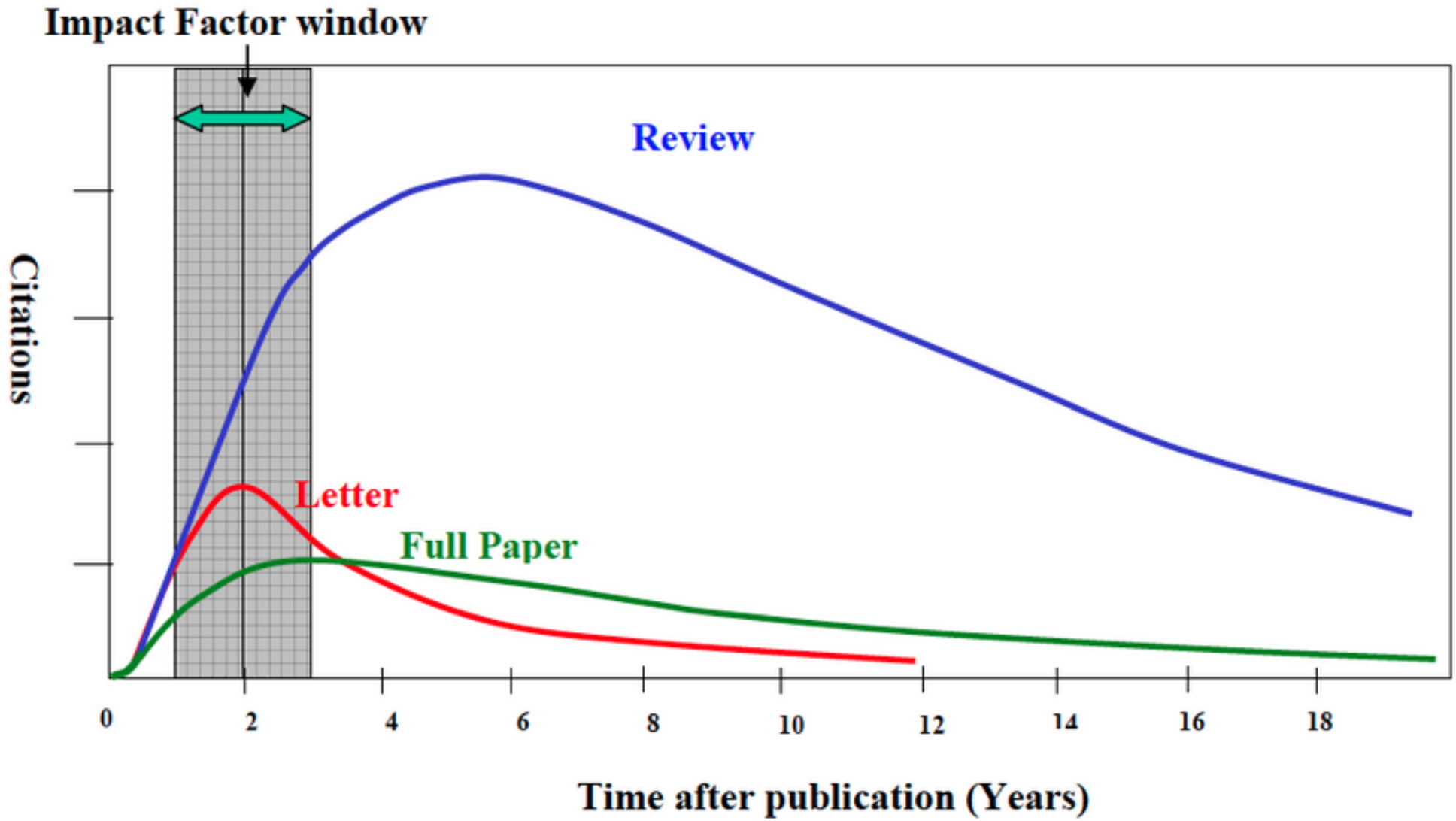

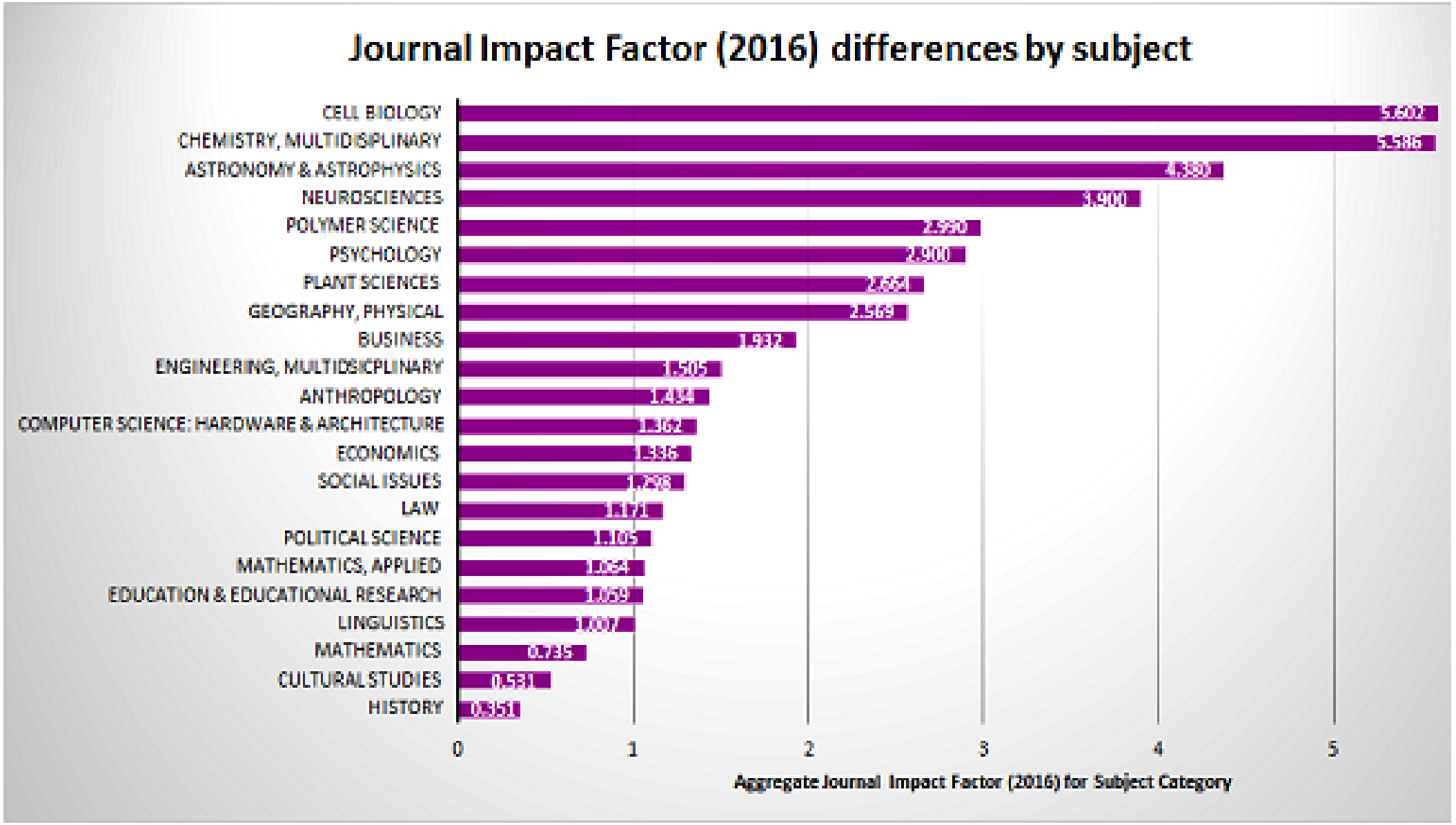
Journal Impact Factor (2016) differences by subject
CELL BIOLOGY
CHEMISTRY, MULTIDISIPLINARY
ASTRONOMY & ASTROPHYSICS
NEUROSCIENCES
POLYMER SCIENCE
PSYCHOLOGY
PLANT SCIENCES
GEOGRAPHY, PHYSICAL
BUSINESS
ENGINEERING, MULTIDSICPLINARY
ANTHROPOLOGY
COMPUTER SCIENCE: HARDWARE & ARCHITECTURE
ECONOMICS
SOCIAL ISSUES
LAW
POLITICAL SCIENCE
MATHEMATICS, APPLIED
EDUCATION & EDUCATIONAL RESEARCH
LINGUISTICS
MATHEMATICS
CULTURAL STUDIES
HISTORY
5.602
5.586
4.550
3.900
2.920
2.900
2.662
2.569
1.937
1.505
1.454
1.362
1.336
1.298
1.171
1.105
1.054
1.049
1.007
0.735
0.581
0.351
0
1
2
3
4
5
Aggregate Journal Impact Factor (2016) for Subject Category

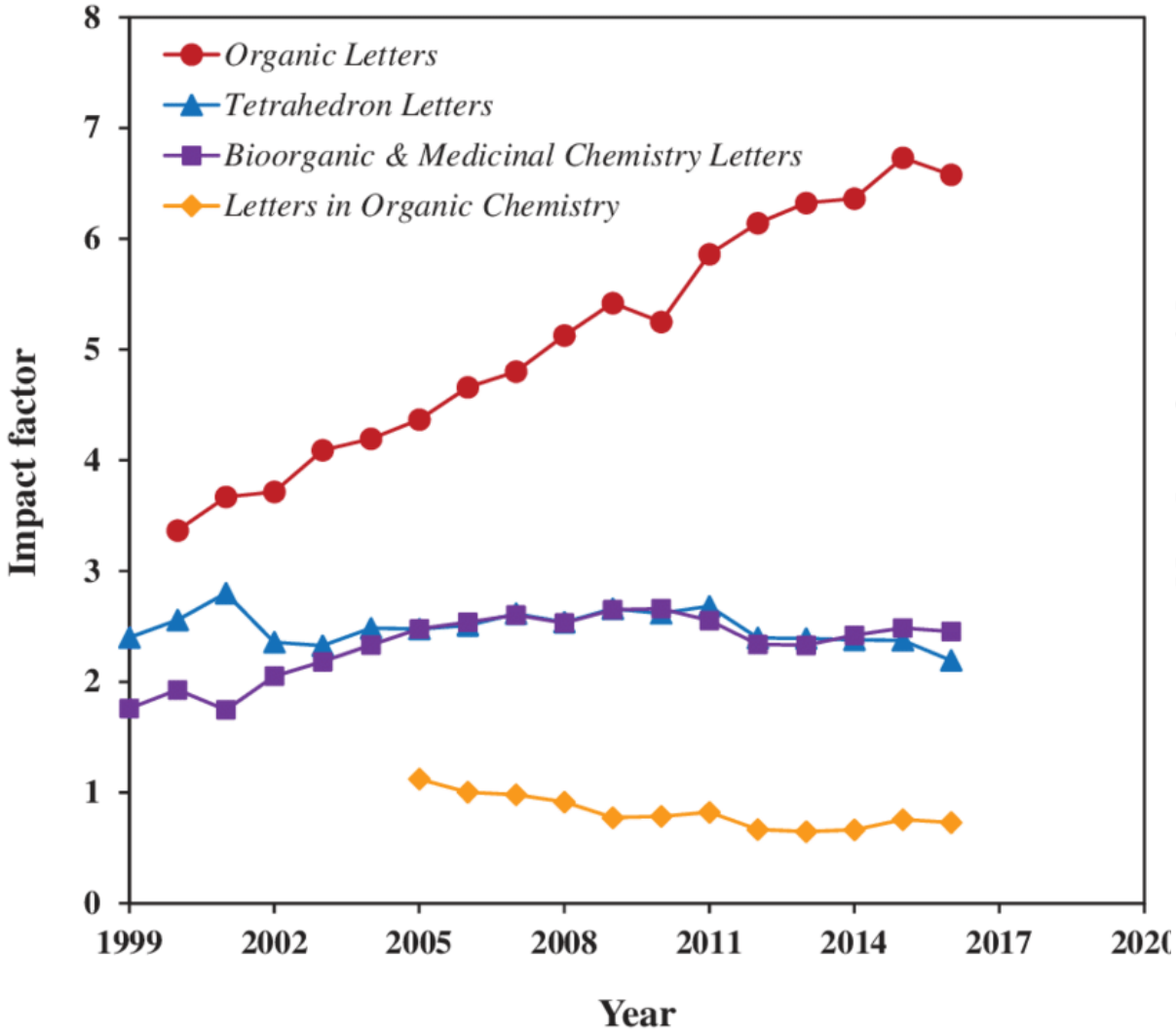

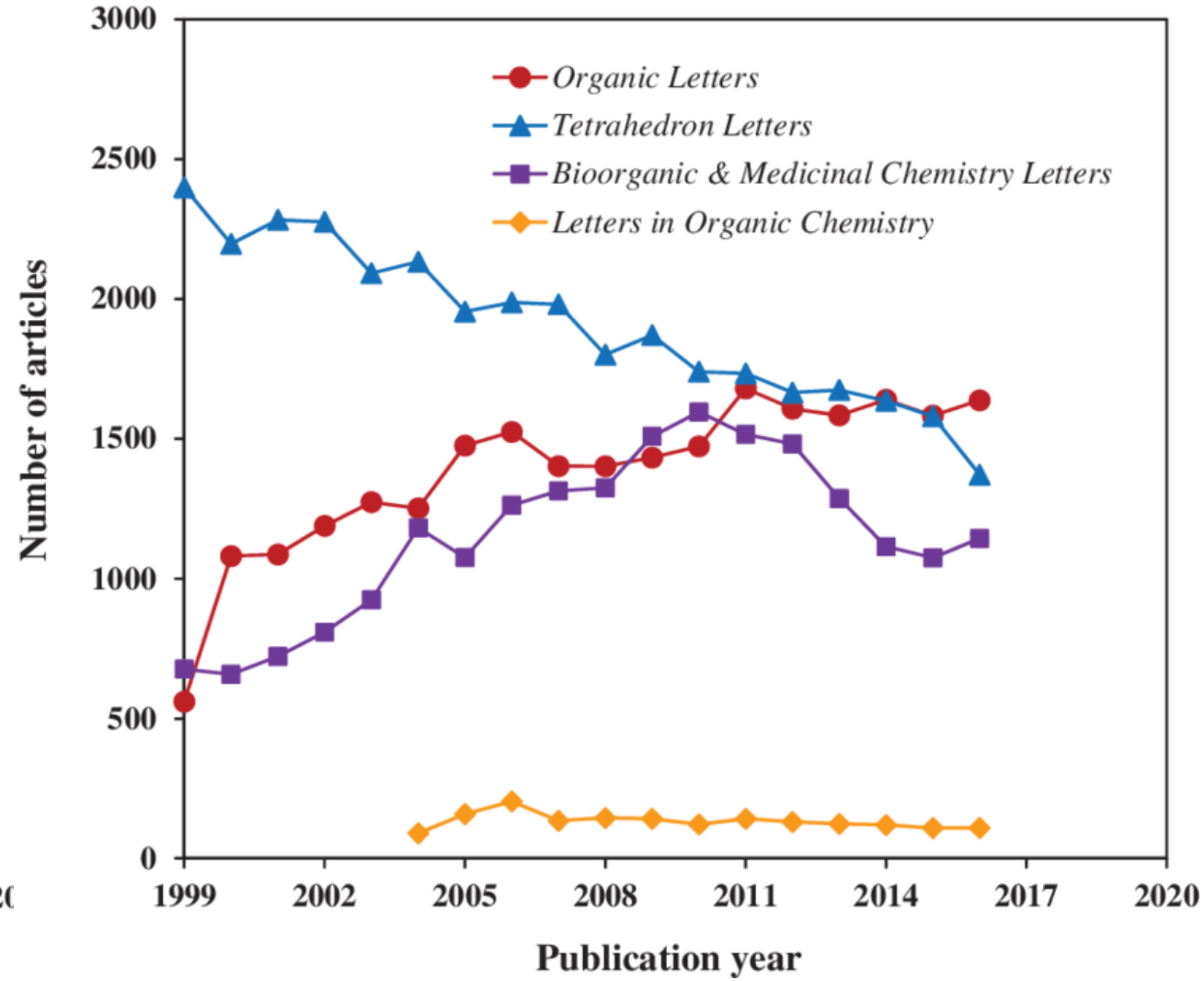

імпакт-фактор змінюється в часі

кореляція незначна
кількість статей впливає

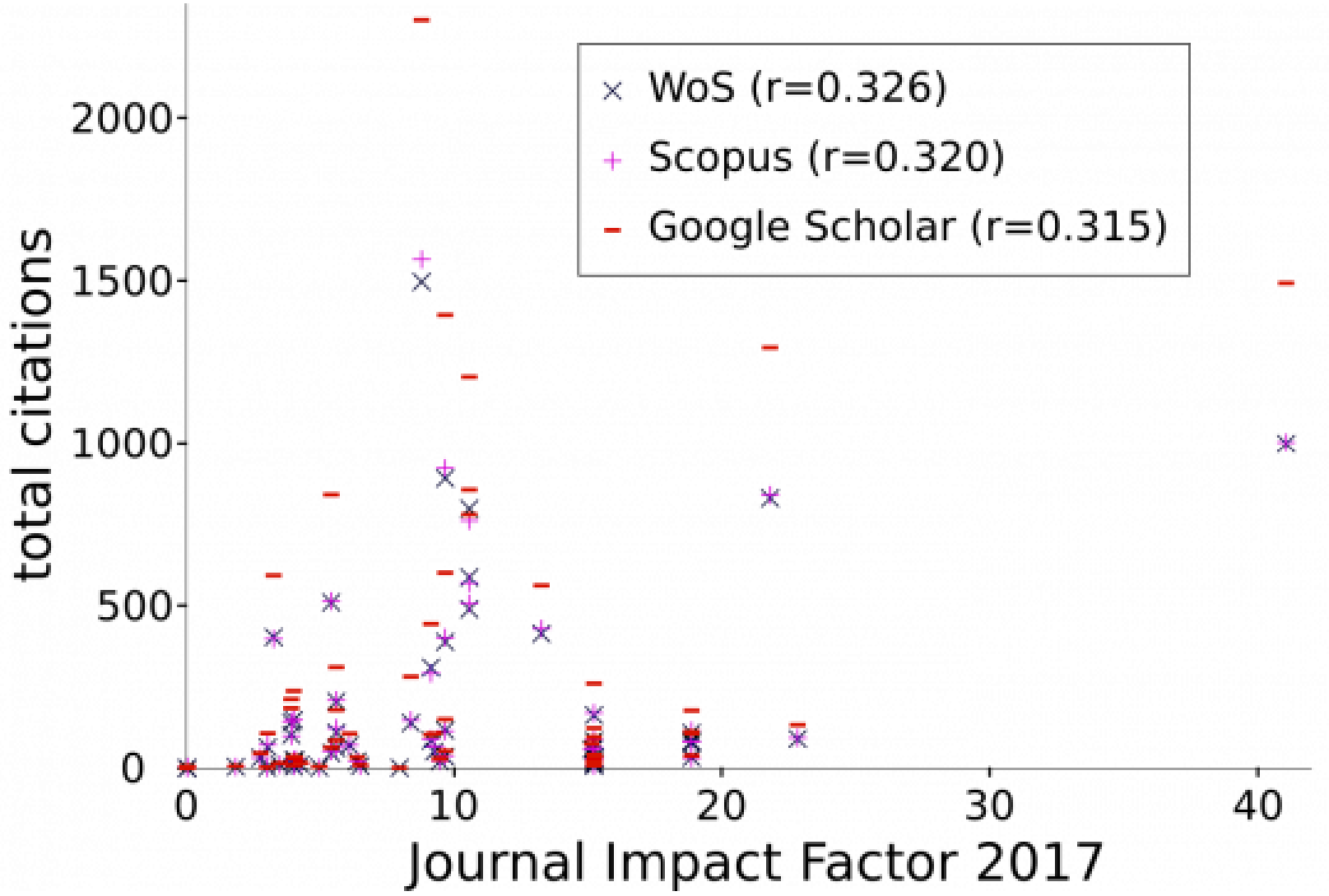

Gold Open Access

- Immediate access the Version of Record (VoR) of a publication via the publishers platform in exchange for payment of a Article Publication Charge (APC); usually free of many conventional licensing and copyright restrictions

Green Open Access

- Access without payment to a version of the publication (not VoR) via a repository, often after an embargo period

Open Access

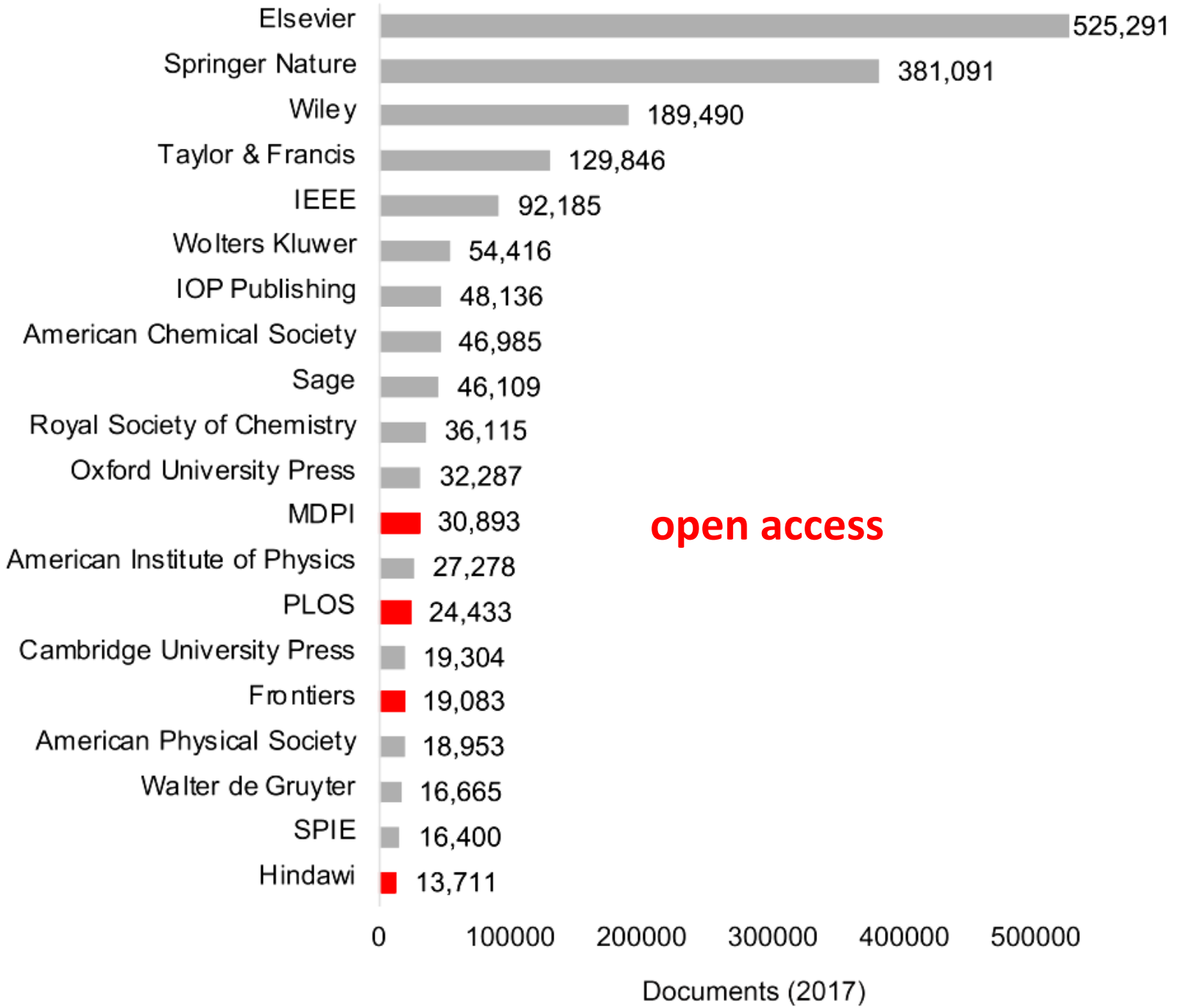
Elsevier
525,291
Springer Nature
381,091
Wiley
189,490
Taylor & Francis
129,846
IEEE
92,185
Wolters Kluwer
54,416
IOP Publishing
48,136
American Chemical Society
46,985
Sage
46,109
Royal Society of Chemistry
36,115
Oxford University Press
32,287
MDPI
30,893
American Institute of Physics
27,278
PLOS
24,433
Cambridge University Press
19,304
Frontiers
19,083
American Physical Society
18,953
Walter de Gruyter
16,665
SPIE
16,400
Hindawi
13,711
open access
0
100000
200000
300000
400000
500000
Documents (2017)

SCImago country ranking

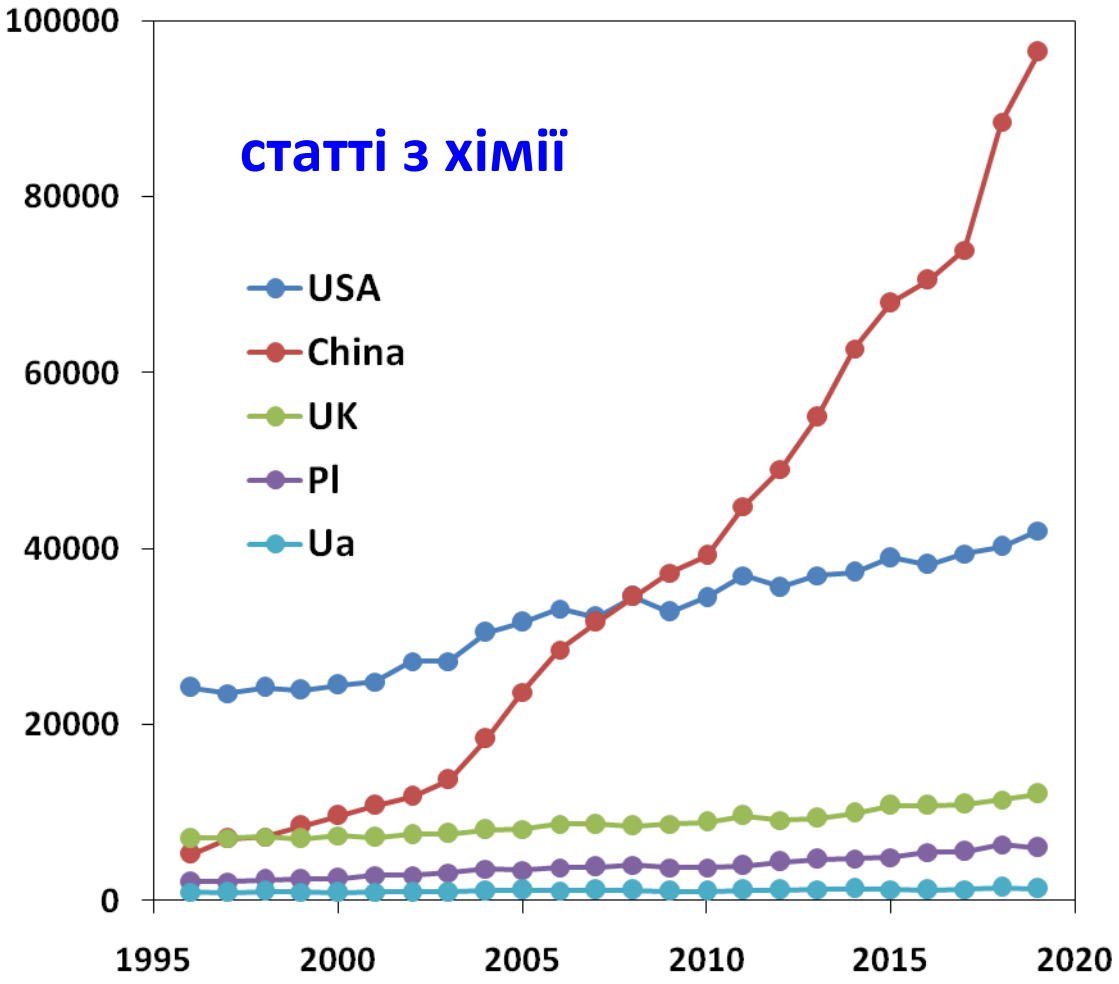

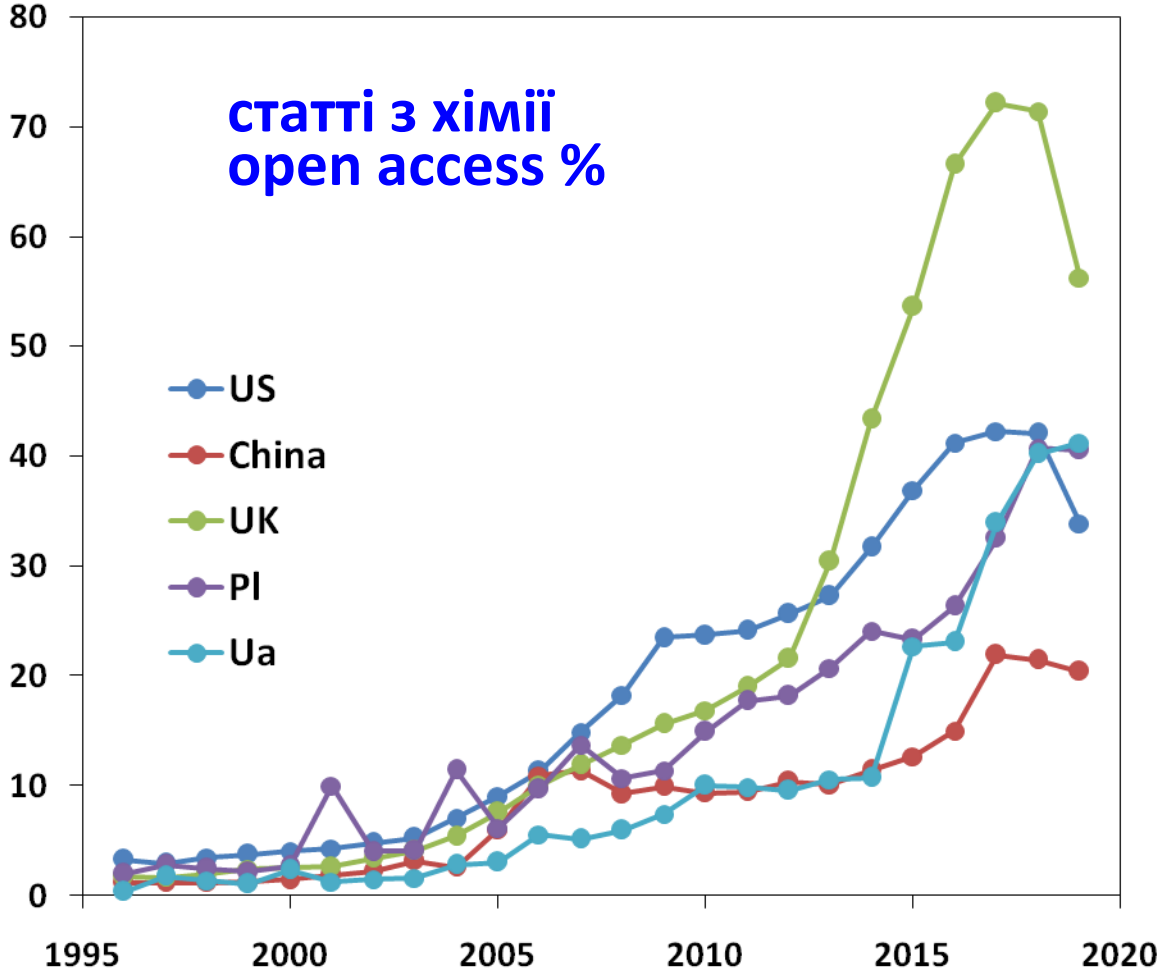

Шийчук 2020

Opportunity to correspond directly with the journal editor.

- Will not be rejected if bad
  - Might leave a bad impression
- Good cover letter may accelerate the editorial process

Another opportunity to advertise your research

- Don't summarize the manuscript
- Don't repeat the abstract
- Show the big picture including the background
  - How is it special and/or worthwhile to the journal?
- Mention why the manuscript is original and what your purpose is
  - Very briefly explain
    - What was done and what was found
    - How will this interest the readers?

The cover letter

CREATIVE SELF-MARKETING; YOU'RE DOING IT WRONG

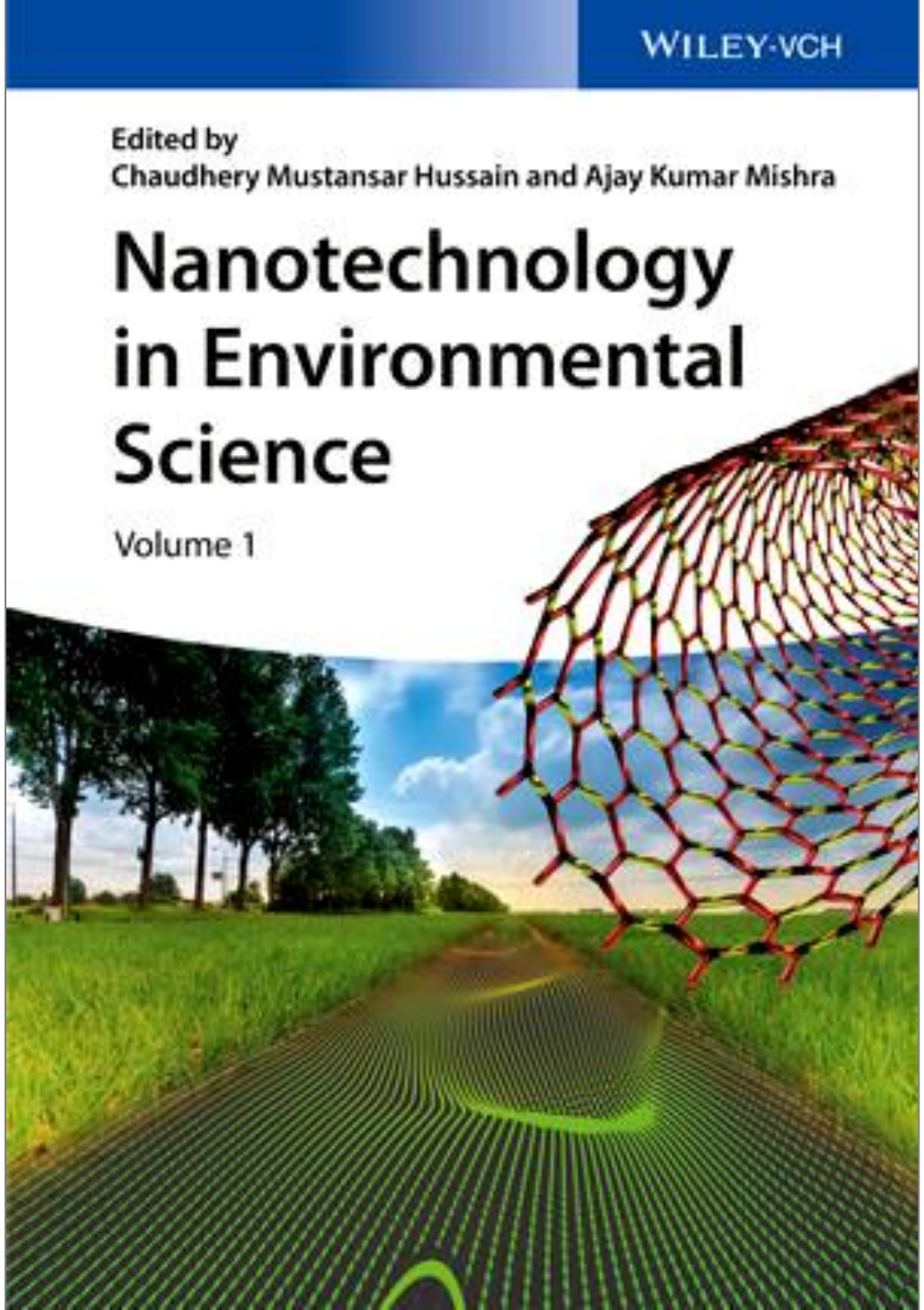

8

Photocatalysis: Activity of Nanomaterials

Tetiana Tatarchuk,[1] Amalthi Peter,[2] Basma Al-Najar,[3] Judith Vijaya,[2] and Mohamed Bououdina[3]

[1]*Vasyl Stefanyk Precarpathian National University, Department of Theoretical and Applied Chemistry, 57, Shevchenko Str., Ivano-Frankivsk 76018, Ukraine*
[2]*Loyola College, Department of Chemistry, Catalysis and Nanomaterials Research Laboratory, Nelson Manickam Road, Chennai, Tamil Nadu 600034, India*
[3]*University of Bahrain, Department of Physics, PO Box 32038, Sakhir, Kingdom of Bahrain*

8.1 Nanomaterials for Photocatalysis

In the past few years, nanomaterials have emerged as one of the main influencers in technology and biomedicine. The extremely small size of nanomaterials (5–100 nm) owe them miraculous properties due to their large surface area in addition to quantum confinement. It is well known that nanomaterials can be shaped in many forms as rods, thin films, powder, and so on [1,2]. They also can be synthesized through several methods resulting in different shapes, sizes, and properties [3]. Therefore, they are applied in mostly every life sector including drugs and modifications, manufacturing, and materials, environmental issues, electronics, energy production, and industry [4]. The photocatalysis process using the unique properties of nanomaterials has been applied in a wide range of applications such as degradation of pollutants from atmosphere and water. It is also used in producing energy. Some nanomaterials such as oxides [5–7], semiconductors [8,9], metals [10,11], and graphene [12,13] have shown great effect on photocatalysis processes [14,15] due to their enhanced and controllable optical properties, which makes them excellent photocatalysts. This chapter will discuss the mechanism of photocatalysis processes using nanomaterials and their applications. Table 8.1 shows some of the nanoparticles applied for photocatalytics procedures. The chapter will also focus on the different types of nanomaterials used in photocatalysis in terms of their synthesis method, microstructure, and their optical and magnetic properties.

Nanotechnology in Environmental Science, First Edition. Edited by Chaudhery Mustansar Hussain and Ajay Kumar Mishra.

Table 8.1 Some of the nanoparticles applied in photocatalytic procedures.

Nanoparticles	Irradiation	Mechanism of photocatalysis enhancement	Reference
TiO_2/WO_3	Sun light/solar UV–visible light	Heterogeneous	[15]
ZnO/Ag	UV (320–400 nm)	Heterogeneous/SPR	[5]
WO_3/TiO_2	UV (365 ± 5 nm)	Heterojunctional-electrical layered system	[6]
p-type -FeOOH/n-type $WO_3{\cdot}H_2O$	UVA (365 nm)	Semiconductors	[16]
Zinc and copper co-doped WO3	Visible light (>420 nm)	Heterogeneous	[17]
N-TiO_2	Visible light	Doping	[18]
Fe-doped response TiO_2 film	Visible light	Doping	[19]
Graphitic carbon nitride (g-C_3N_4) with graphene oxide (GO)	Visible light	Heterogeneous	[12]
TiO_2/graphene oxide (GO) composite nanofibers	Visible light	Heterogeneous	[13]
Gold-doped PdO NPs	(UV) 254 nm	"UV + H_2O_2" system batch system	[20]
Ag NPs on Cd(II) boron imidazolate	UV	SPR	[10]
Ag NPs	UV	SPR	[21]
Ag-polymer core-shell NPs	UVA	SPR	[11]
Gd-doped PbSe NPs	Visible light irradiation	Doping	[8]
$M_xBi_{2-x}Ti_2O_7$ (M: Fe, Mn)	UV light (≥320 nm) Visible light (≥ 400 nm)	Heterogeneous	[9]
Ni-doped CuS	Visible light	Doping	[22]
Na-doped ZnO	Solar irradiation	Doping	[23]

8.2 Mechanism of Photocatalysis

Photocatalysis is a series of chemical reactions that is usually induced by electromagnetic irradiation. This will cause excitation of atoms of the irradiated materials that results in radicals that affect surroundings [5]. Photocatalysis process can be divided into two main stages: reduction and oxidation [24]. When a material is irradiated with photons with energy equal to or higher

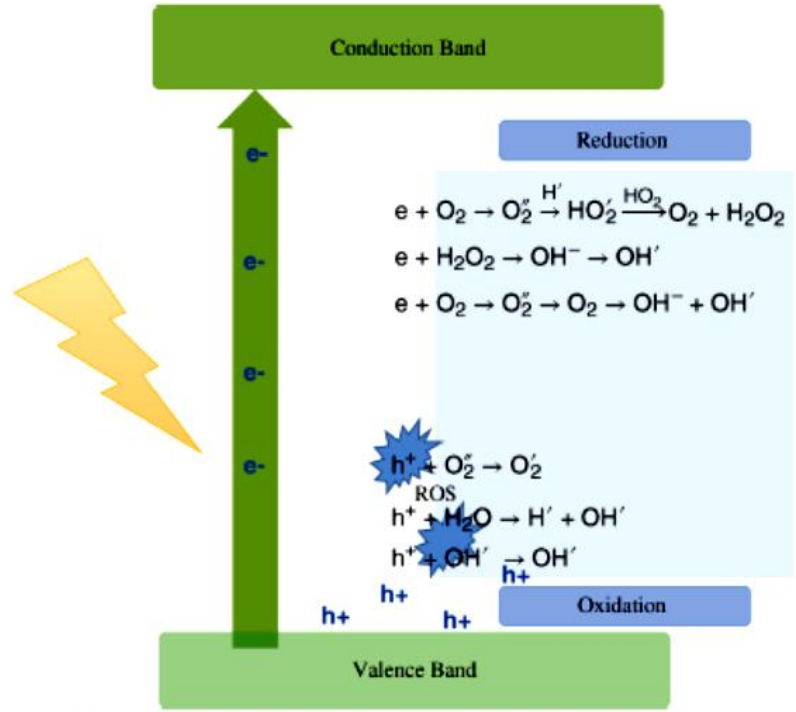

Figure 8.1 Mechanism of photocatalytics process including chemical reactions.

than its bandgap, electrons in the conduction band (CB) will jump to the valence band (VB) through the bandgap leaving positive holes, and this stage is called reduction (Figure 8.1). As a result of reduction, the generated electrons and holes lead to the formation of reactive oxygen spices (ROS) such as O_2 and OH (oxidation). The kind of ROS depends on the type of material and irradiated photons. A typical photcatalysis process is shown in Figure 8.1. The formation of ROS is the significant outcome of photocatalysis, as it can cause various effects such as degradation of dye [10] and antibacterial activity [20]. Other applications of photocatalytic activity are mentioned in Table 8.2. A series of chemical effects occur as a result of photocatlysis. Figure 8.1 shows example of chemical reactions occurs during photocatalysis process.

Efficiency of photocatalysis process can be evaluated by its effect on the surroundings such as degradation, adoption, reduction, or antibacterial activity. The common way of evaluating the efficiency of the photocatalytic process is to compare between the initial concentration of the unwanted substances with the concentration of these substances after the photocatalytic reactions using the following equation:

$$\ln\frac{C_0}{C_t} = kt,$$

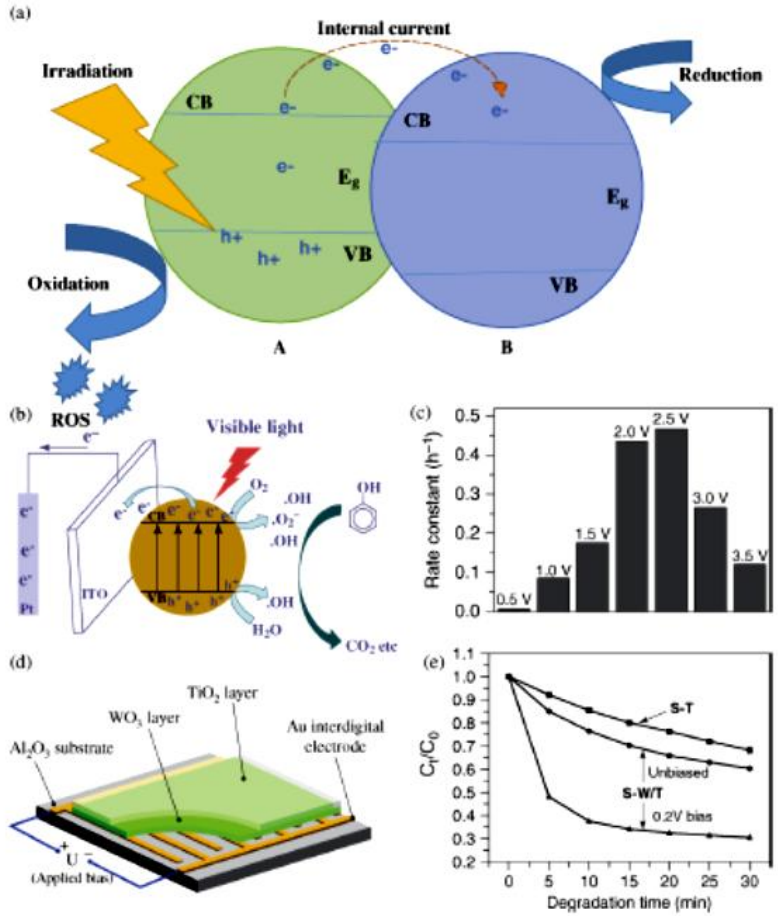

Figure 8.2 (a) Mechanism of hetrostructure photocatalysis. (b) PEC degradation mechanism of phenol by g-C3N4 film electrode [30] (c). The rate constants for EC degradation activity of g-C_3N_4 film electrode for phenol at various potentials in 0.1 M Na_2SO_4 solution (reproduced with permission from Ref. [30]. Copyright 2016, Elsevier). (d) Schematic diagram of the interdigital electrode/WO_3/TiO_2 HEL system (Al_2O_3 substrate, Au interdigital electrode layer, WO_3 layer, and TiO_2 layer from bottom to top) [6]. (e) Comparison of photocatalytic decomposition rates of toluene between S-T and S-W/T with no bias and 0.2 V bias (reproduced with permission from Ref. [6]. Copyright 2011, Elsevier).

found that voltage applied did not dramatically affect the degradation rate. In general, it has been stated that phoroelectrocatlysis not only reduces recombination but also allows electrochemical oxidation that significantly increases the photogedradation rate [31].

Another effective way to decrease the recombination rate is the use of heterogeneous structure (a mixture of different materials) [24]. This allows

8.3 Synthesis of Photocatalytic Materials

Numerous methods have been established in the synthesis of photocatalytic materials during the past decade because of their applications in processes such as wastewater and effluents treatment [36], which includes degradation of organic dyes [37] and volatile organic compounds [38], antimicrobial, antibacterial, and antioxidant activity [39], solar cell applications [40], photocatalytic self cleaning effect [41], hydrogen generation [42], food packaging [43], and biomedical and medical applications [44].

Numerous studies have explained that the intrinsic properties of photocatalytic materials can be effectively tailored by controlling their size, shape, composition, crystallinity, and structure. The growth of nanoscale materials rely on factors such as their thermodynamic and kinetic barriers in the reaction. It is also influenced by vacancies, defects, and surface reconstruction. Most synthetic methods for synthesizing nanomaterials use conventional heating due to the need for high-temperature-initiated nucleation followed by a controlled addition of precursor to the reaction.

The preparation of photocatalytic nanocomposite materials can be ideally divided into three main steps: (i) synthesis of an effective photocatalyst, (ii) its surface functionalization to enhance reactivity, and (iii) its incorporation in the most suitable host matrix according to the final application. Various methods have been developed for the synthesis of these property-tailored materials, which include hydrothermal, coprecipitation, sol–gel, ultrasonic impregnation, ionic liquid-assisted photochemical synthesis, electrochemical synthesis, solvotherml, facile chemical impregnation, microwave-assisted synthesis, and so on. In this section, recent progress in modern material science for the synthesis of photocatalytic materials, as well as advances achieved in their functionalization to tune their surface chemistry, will be presented and discussed. The next section focuses on the various nanoparticles that are employed in a wide range of applications of photocatalysis, see Figure. 8.5.

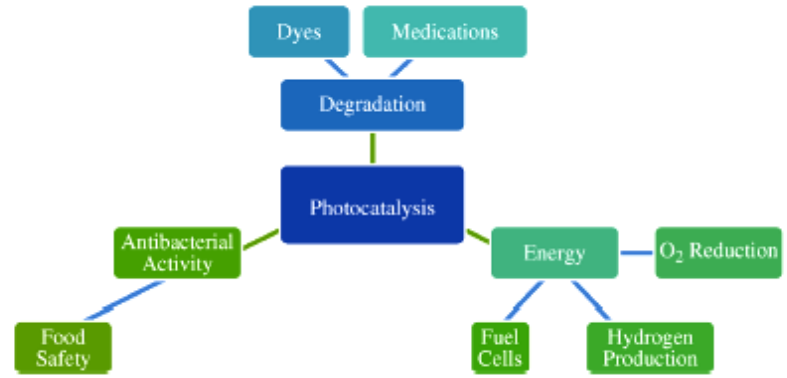

Figure 8.5 Photocatalysis applications of nanomaterials.

that the Bi_5O_7I can be obtained from the BiOI precursor at lower temperatures. XPS wide scan spectra of the samples indicate the presence of bismuth (Bi 4f, Bi 4d, Bi 4p, and Bi 5d), oxygen (O 1s), iodine (I 3d), and carbon (C 1s). The observed shift of binding energies confirms the complete phase transition from BiOI to Bi_5O_7I after heat treatment at 450 °C. SEM and TEM show spherical microstructures assembled by numerous ultrathin nanosheets. For all BiOI powders, the spherical shape is maintained and their diameters slightly decreased from 3 to1.5 mm, while the thickness of the sheet-like nanostructures increased. TEM image of a single Bi_5O_7I microsphere heat treated at 450 °C confirms it is composed of nanosheets of a thickness of about 25 nm. HR TEM image reveals that the two different lattice fringes with intervals of about 0.317 and 0.306 nm can be assigned to (312) and (113) planes of the orthorhombic phase Bi_5O_7I, respectively. The BiOI-400 sample showed the higher adsorption property with RhB that is attributed to its large surface area, unique surface, and surface electronegativity (see Figure 8.12) [149].

8.4.5 Phase Transition Studies of Bicrystalline Cr-TiO_2 Nanoparticles

Employing one-step flame spray pyrolysis technique, Tian *et al.* [150] synthesized bicrystalline phase Cr-TiO_2 nanoparticles. The mixed phases of TiO_2, such as anatase/rutile and anatase/brookite, exhibit higher photocatalytic activity than pure single-crystal phase. The enhanced activity of mixed phases is attributed to the formation of heterojunction between different phases, which can efficiently separate the spatial charges and consequently improve the quantum yield of TiO_2. The intimate contact between two phases is necessary to enhance the

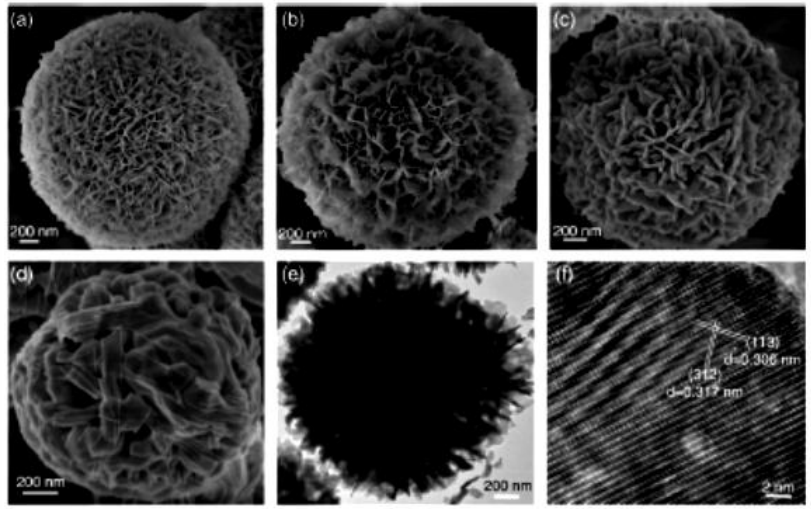

Figure 8.12 SEM images of pure (a) and heat-treated BiOI powders at 400 (b), 450 (c), and 500 °C (d). TEM (e) and HRTEM (f) images of the BiOI powder heat treatment at 450 °C (reproduced with permission from Ref. [149]. Copyright 2016, Elsevier).

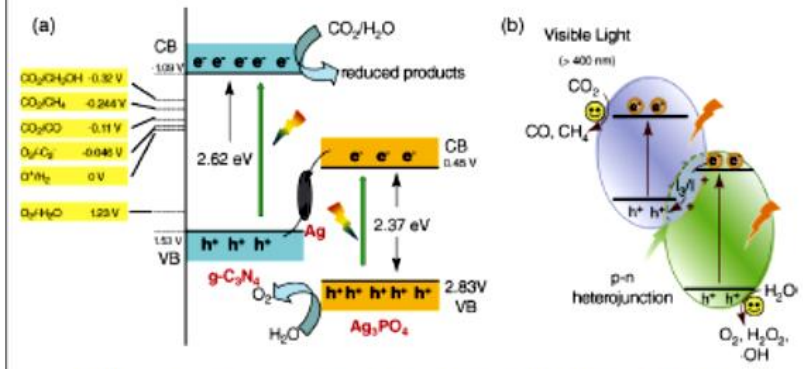

Figure 8.31 Reaction schemes for the photocatalytic reduction of CO_2 with H_2O on (a) Ag_3PO_4/g-C_3N_4 composite (reproduced with permission from Ref. [310]. Copyright 2015, American Chemical Society) and on (b) BiOI/g-C_3N_4 photocatalysts (reproduced with permission from Ref. [313]. Copyright 2016, American Chemical Society).

bismuth oxyhalides (BiOX, X = Br, I) [312–314], and so on have also been reported as photocatalysts for effective CO_2 reduction. For example, a combination of the g-C_3N_4 with other proper semiconductors such as Ag_3PO_4 (Figure 8.31a) and BiOI (Figure 8.31b) not only extend the visible-light absorption capacity but also improve the separation of electron–hole pairs. It provides a great enhancement of the photocatalytic activity for different hybrids and will undoubtedly help in the development of the next generation of photocatalysts for environmental applications.

References

1 Mao-Yuan, C. and Heh-Nan, L. (2015) Enhanced photocatalysis of ZnO nanowires co-modified with cuprous oxide and silver nanoparticles. *Mater. Lett.*, **160**, 440–443.

2 Sun, G., Zhu, C., Zheng, J., Jiang, B., Yin, H., Wang, H., Qiu, S., Yuan, J., Wu, M., Wu, W., and Xue, Q. (2016) Preparation of spherical and dendritic CdS@TiO2 hollow double-shelled nanoparticles for photocatalysis. *Mater. Lett.*, **166**, 113–115.

3 Richter, R., Ming, T., Davies, P., Liud, W., and Caillo, S. (2017) Removal of non-CO_2 greenhouse gases by largescale atmospheric solar photocatalysis. *Prog. Energy Combust. Sci.*, **60**, 68–96.

4 Khan, I., Saeed, K., and Khan, I. (2017) Nanoparticles: properties, applications and toxicities. *Arabian J. Chem.* doi: http://dx.doi.org/10.1016/j.arabjc.2017.05.011

5 Andrade, G.R.S., Nascimento, C., Lima, Z.M., Teixeira-Neto, E., Luiz, P., Iara, Costac, and Gimeneza, F. (2017) Star-shaped ZnO/Ag hybrid nanostructures for enhanced photocatalysis and antibacterial activity. *Appl. Surf. Sci.*, **399**, 573–582.

307 Baran, T., Wojtyła, S., Dibenedetto, A., Aresta, M., and Macyk, W. (2015) Zinc sulfide functionalized with ruthenium nanoparticles for photocatalytic reduction of CO_2. *Appl. Catal. B*, **178**, 170–176.

308 Zhu, Z., Qin, J., Jiang, M., Ding, Z., and Hou, Y. (2017) Enhanced selective photocatalytic CO_2 reduction into CO over Ag/CdS nanocomposites under visible light. *Appl. Surf. Sci.*, **391**, Part B, 572–579.

309 Ye, S., Wang, R., Wu, M.-Z., and Yuan, Y.-P. (2015) A review on g-C_3N_4 for photocatalytic water splitting and CO_2 reduction. *Appl. Surf. Sci.*, **358**, Part A, 15–27.

310 He, Y., Zhang, L., Teng, B., and Fan, M. (2015) New application of Z-scheme Ag_3PO_4/g-C_3N_4 composite in converting CO_2 to fuel. *Environ. Sci. Technol.*, **49** (1), 649–656.

311 Dai, W., Xu, H., Yu, J., Hu, X., Luo, X., Tu, X., and Yang, L. (2015) Photocatalytic reduction of CO_2 into methanol and ethanol over conducting polymers modified Bi_2WO_6 microspheres under visible light. *Appl. Surf. Sci.*, **356**, 173–180.

312 Bai, Y., Ye, L., Chen, T., Wang, P., Wang, L., Shi, X., and Wong, P.K. (2017) Synthesis of hierarchical bismuth-rich $Bi_4O_5Br_xI_{2-x}$ solid solutions for enhanced photocatalytic activities of CO_2 conversion and Cr(VI) reduction under visible light. *Appl. Catal. B*, **203**, 633–640.

313 Wang, J.-C., Yao, H.-C., Fan, Z.-Y., Zhang, L., Wang, J.-S., Zang, S.-Q., and Li, Z.-J. (2016) Indirect Z-scheme BiOI/g-C_3N_4 photocatalysts with enhanced photoreduction CO_2 activity under visible light irradiation. *ACS Appl. Mater. Interfaces*, **8** (6), 3765–3775.

314 Ye, L., Jin, X., Ji, X., Liu, C., Su, Y., Xie, H., and Liu, C. (2016) Facet-dependent photocatalytic reduction of CO_2 on BiOI nanosheets. *Chem. Eng. J.*, **291**, 39–46.

SCI-HUB

...to remove all barriers in the way of science

the first website in the world to provide mass & public access to research papers

enter URL, PMID / DOI or search string

open

about ideas community donate

Plagiarism: the main types

Direct Plagiarism

- Word-for-word transcription without attribution

Self Plagiarism

- Borrows generously from the writer's previous work without citation

Mosaic Plagiarism

- Paraphrases from multiple sources, made to fit together and contains almost no original work

Accidental Plagiarism

- Neglects to cite sources, or misquotes their sources or unintentionally paraphrases sources without attribution